Marine Biology (2020) 167:146
https://doi.org/10.1007/s00227-020-03754-2

ORIGINAL PAPER

Regional environmental drivers of Kemp's ridley sea turtle somatic growth variation

Matthew D. Ramirez[1,6] · **Larisa Avens**[2] · **Lisa R. Goshe**[2] · **Melissa L. Snover**[3] · **Melissa Cook**[4] · **Heather L. Haas**[5] · **Selina S. Heppell**[1]

Received: 13 March 2020 / Accepted: 8 August 2020

Abstract

Many environmental processes influence animal somatic growth rates. However, elucidating specific drivers of somatic growth variation has been challenging for marine megafauna. Using a 20+ year dataset of somatic growth generated through skeletochronology, we evaluated the relationship between multiple region-wide environmental factors—the Deepwater Horizon (DWH) oil spill, increasing population density, and climate variability—and age- and region-specific Kemp's ridley sea turtle (*Lepidochelys kempii*) somatic growth. We observed significant, multi-year reductions in mean oceanic (age 0) and small neritic (age 2–5) juvenile growth rates beginning in 2012 for turtles stranded along the U.S. Gulf of Mexico (GoM) and Atlantic Coasts, which resulted in a reduction in mean size-at-age. We hypothesize that this growth decline is related to long-term deleterious effects of the DWH oil spill on neritic and oceanic food webs in the GoM. Additionally, regional climate indices were strongly correlated with oceanic juvenile growth with a 2-year lag (cross-correlation = –0.57 to 0.60), whereas GoM small neritic juvenile growth was strongly related to population abundance metrics. Generalized additive models that included all examined environmental covariates indicated that the drivers of the 2012 growth rate decline had the strongest effect on Kemp's ridley growth rates between 1995 and 2015, but that additive or synergistic effects of both climate variability and changing population abundance are likely for certain life stages. Continued collection of sea turtle humeri is needed to further clarify mechanisms underpinning the observed growth patterns given the coincidental timing of changes in environmental parameters examined herein.

Responsible Editor: P. Casale.

Reviewers: D. Shaver and B. Wallace.

Electronic supplementary material The online version of this article (https://doi.org/10.1007/s00227-020-03754-2) contains supplementary material, which is available to authorized users.

✉ Matthew D. Ramirez
mdramirez@uri.edu

[1] Department of Fisheries and Wildlife, Oregon State University, Corvallis, OR 97331, USA

[2] NOAA National Marine Fisheries Service, Southeast Fisheries Science Center, Beaufort Laboratory, Beaufort, NC 28516, USA

[3] Population Ecology Services, Pago Pago 96799, American Samoa

[4] NOAA National Marine Fisheries Service, Southeast Fisheries Science Center, Pascagoula, MS 39567, USA

[5] Northeast Fisheries Science Center, NOAA National Marine Fisheries Service, Woods Hole, MA 02543, USA

[6] 215 South Ferry Road, Narragansett, RI 02889, USA

Introduction

A suite of natural and anthropogenic stressors have reshaped marine ecosystems over the past century through cascading effects on animal populations and the habitats which they occupy (Halpern et al. 2008; Rocha et al. 2014; McCauley et al. 2015). Numerous studies have characterized single stressor effects on marine species, but fewer have examined species response to cumulative or integrative effects of multiple environmental factors, particularly in long-lived, higher order marine megafauna (Crain et al. 2008; Bjorndal et al. 2013). As the population dynamics of long-lived species are highly sensitive to small changes in demographic rates (Heppell et al. 2000), increasing insight into environmental effects on growth, survival, and reproduction may help to improve understanding of population and community dynamics, and ultimately aid the development of conservation and management plans for protected species. Moreover, disentangling the relative influence of myriad environmental stressors on animal populations and ecosystems is essential to predicting future ecosystem response to perturbation. Sea turtles provide an ideal system to investigate the influence of multiple environmental phenomena on demographic rates, because most species retain annual records of somatic growth in their humerus bones, similar to growth rings in trees and otoliths in fish, that can be collected from dead stranded turtles (Avens and Snover 2013). And, as ectotherms, their growth rates are also highly influenced by environmental conditions.

The critically endangered Kemp's ridley sea turtle (*Lepidochelys kempii*) is a particularly appealing model species to evaluate environmental drivers of somatic growth rates. First, humerus bones have been collected from dead stranded turtles since the early 1990s (Snover and Hohn 2004; Avens et al. 2017), providing a unique sample set for growth analysis. Second, their global distribution is largely restricted to the Gulf of Mexico (GoM) and U.S. Atlantic (Musick and Limpus 1997), areas that are experiencing rapid environmental change including a climate-driven ecological regime shift in the 1990s (Sanchez-Rubio et al. 2011; Karnauskas et al. 2015) and the 2010 Deepwater Horizon (DWH) oil spill (DWH NRDA Trustees 2016). Following a 1–3-year oceanic life stage primarily occurring in the GoM (TEWG 2000; Avens et al. in review), turtles recruit to neritic habitats in either the GoM or U.S. Atlantic Coast (NMFS and USFWS 2015). Although migration from neritic GoM to U.S. Atlantic Coast habitats is possible (Renaud and Williams 2005), these migrations appear rare and it is presumed that these population subgroups largely remain isolated from one another until Atlantic Kemp's ridleys return to the GoM at or near maturity (Caillouet et al. 2015). This geographic isolation of two components of the population provides a natural experiment to examine DWH oil spill effects on sea turtle growth rates and potentially separate them from other region-wide environmental stressors. Finally, the Kemp's ridley population grew exponentially (12–16% per year) through the 1990s and 2000s following decades of successful conservation and management (NMFS and USFWS 2015). This population growth, combined with a robust record of nest and hatchling production for nearly the entire species, provides the opportunity to evaluate density-dependent effects on somatic growth rates (Caillouet et al. 2016, 2018).

Environmental impacts of the DWH oil spill and impact mitigation efforts were unprecedented in their spatiotemporal and ecological scale (DWH NRDA Trustees 2016; Beyer et al. 2016; Berenshtein et al. 2020). Negative effects of the DWH oil spill on somatic growth rates have been documented in a wide range of fish and invertebrate species (e.g., Rozas et al. 2014; Brown-Peterson et al. 2016; Herdter et al. 2017; Perez et al. 2017). Although DWH impacts on marine megafauna demographic rates are less understood, they remain a significant concern given the continued deterioration of the health of GoM bottlenose dolphins and the clear decadal impacts of the 1989 Exxon Valdez oil spill on marine ecosystems and animal demographic rates (Peterson et al. 2003; Kellar et al. 2017). Immediate effects on sea turtle survival and physiology are well documented, but otherwise much remains unknown about their response to this anthropogenic disturbance (McDonald et al. 2017; Mitchelmore et al. 2017; Stacy et al. 2017; Wallace et al. 2017). Sublethal or indirect effects of the DWH oil spill on sea turtle health may be responsible for a general decline in nutritional condition of stranded sea turtles since 2012 and a reduction in juvenile Kemp's ridley growth rates in Mississippi since 2010 (Stacy 2015; Coleman et al. 2016).

Following decades of conservation and management, the abundance of all Kemp's ridley life stages grew rapidly between 1990 and 2009 (Heppell et al. 2004; NMFS and USFWS 2015). Unexpectedly, annual nest counts have fluctuated widely since 2010 and one hypothesis is that density-dependent processes may be acting on the population (Gallaway et al. 2016; Caillouet et al. 2016, 2018). While the current population is less than 10% of its estimated historic size (Bevan et al. 2016), long-term alteration and degradation of GoM ecosystems, including reductions in important food resources (e.g., blue crab *Callinectes sapidus*; VanderKooy 2013), may have lowered the potential carrying capacity of the GoM for sea turtles and other marine top predators (Heppell et al. 2007; Caillouet 2014). Most support for this hypothesis is derived from analyses of the species' nesting trends (Gallaway et al. 2016; Caillouet et al. 2016, 2018; Kocmoud et al. 2019), which are confounded after 2010 with unknown effects of the DWH oil spill, and the observation of increasing breeding intervals for Kemp's ridleys nesting in Texas from 2008 to 2016 (Shaver et al. 2016). However, other environmental factors, such as colder temperatures on the foraging grounds during the winter of 2009–2010 (Lamont and Fujisaki 2014; Gallaway et al. 2016), may underpin this change in breeding interval and additional investigations are needed to evaluate whether density-dependent processes are influencing Kemp's ridley demographic rates.

Climate variability is a primary driver of spatiotemporal variability in ocean productivity, and abrupt changes in climate often precipitate ecological regime shifts (Rocha et al. 2014). Within the North Atlantic Ocean, an ecological regime shift occurred in the late-1990s as a result of an abrupt warming of the ocean that coincided with one of the strongest El Niño events on record as well as a shift from the cool to warm phase of the Atlantic Multidecadal Oscillation (Sanchez-Rubio et al. 2011; Luczak et al. 2011; Reid and Beaugrand 2012; Beaugrand et al. 2013; Karnauskas et al. 2015). This late-1990s regime shift has been linked to reduced blue crab productivity in the GoM (Sanchez-Rubio et al. 2011), an important food source for sea turtles, as well as declining growth rates in loggerhead (*Caretta caretta*), green (*Chelonia mydas*), and hawksbill (*Eretmochelys imbricata*) sea turtles (Bjorndal et al. 2013, 2016,2017). Similar declines in growth were observed in large juvenile and adult Kemp's ridleys in the GoM from 1988 to 2009 and small juveniles from 2004 to 2009 (Avens et al. 2017), although links to climate variability have yet to be evaluated.

Here, we examined temporal trends in juvenile Kemp's ridley sea turtle somatic growth rates using a 20+ year dataset generated through skeletochronology. The primary objective of this study was to quantify the relative influence of multiple regional environmental stressors—the DWH oil spill, increasing population density, and climate variability—on sea turtle growth rates. We developed and tested a suite of hypotheses related to the differential effect of these factors that are outlined here and in Fig. 1. Given a significant degradation of offshore and nearshore habitats in the GoM following the 2010 DWH oil spill and the observed decline in GoM-stranded turtle nutritional condition after 2012 (Stacy 2015; Beyer et al. 2016), we predicted that Kemp's ridley growth rates would decline following the DWH oil spill for both oceanic and neritic juveniles. We specifically predicted that this change would occur beginning in 2010, because annual Kemp's ridley skeletal growth begins in spring, coincident with the timing of the DWH oil spill. Importantly, we predicted that Atlantic turtle growth rates would not change after 2010 given their spatial isolation from the DWH oil spill. We predicted that density-dependent effects, if present, would result in declining growth rates beginning in the mid- to late-2000s, when population growth was the highest (NMFS and USFWS 2015). We expected density-dependent effects which would primarily manifest in small juvenile life stages in the GoM as they have the fastest growth rates and experience the greatest competition with conspecifics for resources due to their size and relative inexperience. We assumed that Atlantic Kemp's ridleys are not strongly influenced by intraspecific population density due to their relatively low abundance. Finally, we predicted that climate effects would cause declining growth rates across all Kemp's ridley life stages and habitats beginning in the late-1990s in response to a regional regime shift as observed in other western North Atlantic sea turtle species (Bjorndal et al. 2016, 2017).

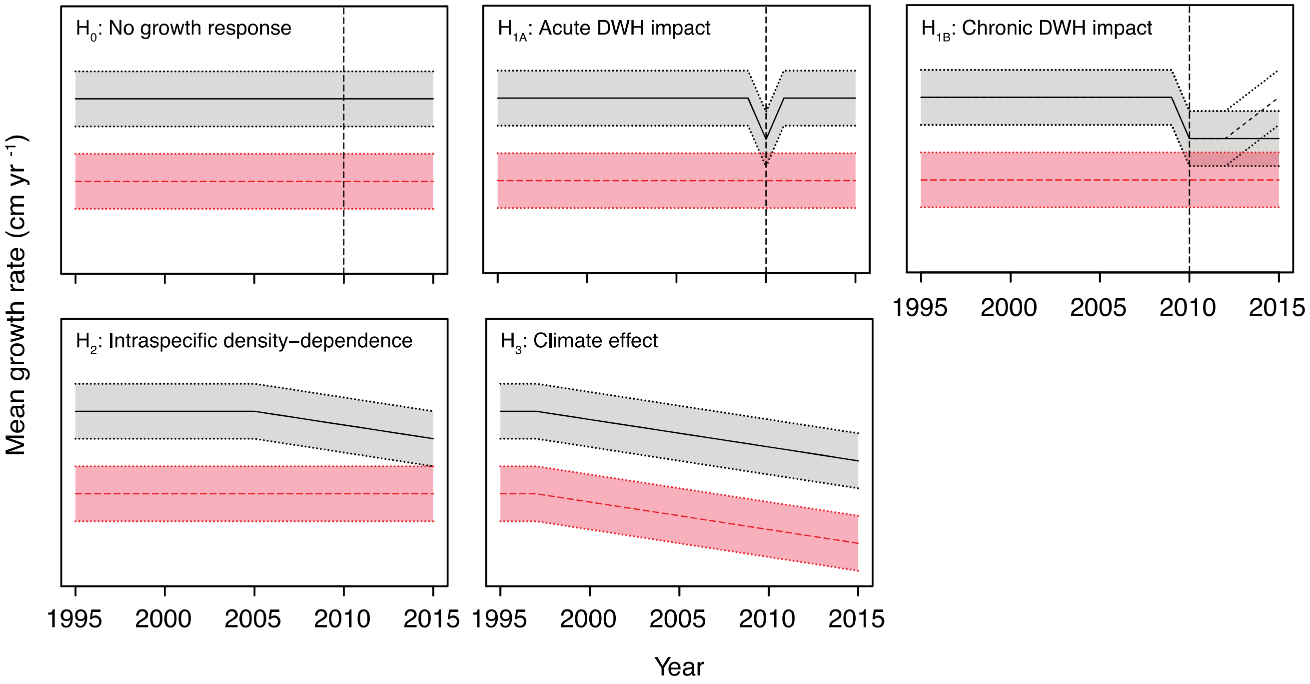

Fig. 1 Conceptual model of alternative hypotheses for the size class-specific growth response of Kemp's ridley sea turtles to environmental factors examined herein. All Kemp's ridleys first reside in oceanic habitats in the central Gulf of Mexico (GoM) for 1–3 years and then recruit to neritic habitats along either the GoM or U.S. Atlantic Coast. The shaded areas represent growth variation for GoM (black lines, gray shading) and Atlantic (red lines, red shading) life stages. Vertical dashed lines identify the year of the Deepwater Horizon (DWH) oil spill (2010). H_0 = no growth response in turtles from either geographic region or life stage to any factor examined. H_1 = acute or chronic DWH oil spill-induced growth response for GoM life stages only (oceanic and neritic); no growth response in Atlantic neritic life stages due to geographic isolation from DWH oil spill, although Atlantic turtles may exhibit a past response during their GoM oceanic life stage. H_2 = density-dependent decline in somatic growth beginning in the mid-2000s during period of exponential population growth; effect in GoM turtles only as > 80% of the population is thought to reside in the GoM (Putman et al. 2013; NMFS and USFWS 2015). H_3 = declining growth beginning in the late-1990s in response to climate-driven ecological regime shift

Materials and methods

Sample collection and processing

Front flippers were collected from Kemp's ridleys that stranded on U.S. beaches by participants of the Sea Turtle Stranding and Salvage Network (Texas to Massachusetts, 1991–2017). Samples were obtained from turtles that either stranded dead or stranded alive, but were later euthanized. Stranding location, date, and carapace length were recorded at the time of stranding (see Tables 1 and S1 for summary). Carapace length was measured as straight-line (SCL) or curved (CCL) carapace length, notch to tip. In cases where only CCL was recorded, CCL was converted to SCL as described by Avens et al. (2017). This study utilizes and extends the growth datasets presented in Avens et al. (2017) ($n = 333$ turtles, GoM) and Snover et al. (2007) ($n = 144$, Atlantic) to include growth histories obtained from a total of 784 turtles stranded along the U.S. GoM Coast and 451 turtles stranded along the U.S. Atlantic Coast. We assume that data derived from these strandings are generally reflective of turtles within each region (GoM vs. Atlatnic), but acknowledge that strandings represent a non-random sampling of the population. The likelihood of a dead turtle stranding is influenced by carcass decomposition rate, drift time, and distance which are influenced by ocean currents and temperature, and potential scavenging by predators. And, the probability of a stranded turtle being documented is influenced by coastline accessibility and public reporting. Combined, turtle strandings are likely biased towards individuals that die closer to the shoreline and in months where temperatures are cooler and decomposition rates are slower. This, perhaps, skews the dataset towards younger/smaller turtles that inhabit more shallow marine habitats and excludes most oceanic stage turtles, though data for this life stage can be retained in the bones of small neritic juveniles.

Humerus bones were prepared and histologically processed as described by Avens and Snover (2013) and Avens et al. (2017). Tissue was removed from the humerus bones, which were then boiled and air dried for at least 2 weeks. A low-speed isomet saw (Buehler) was used to cut a 2–3 mm thick cross-section from each bone just distal to the deltopectoral muscle insertion scar. Bone sections were fixed and decalcified using Cal Ex II (Fisher Scientific) or 10% neutral buffered formalin followed by RDO (Apex Engineering Corporation) and thin sectioned to 25 μm using a freezing-stage microtome (Leica) or cryostat (Thermo Scientific Microm HM 550). Thin sections were stained using diluted Ehrlich's hematoxylin, mounted onto microscope slides in 100% glycerin, and imaged using a digital camera fitted to a compound microscope. Growth mark analyses were performed using image analysis software (Olympus Microsuite and cellSens) and Adobe Photoshop (Adobe Systems). Two or three readers (of L. Avens, L. R. Goshe, M. Ramirez, and M. Snover) independently analyzed the digital bone images to determine the number and placement of lines of arrested growth (LAGs), which delimit the outer edges of each skeletal growth mark (Snover and Hohn 2004), followed by a joint assessment to reach consensus. Once consensus was reached, total humerus section diameter and the diameter of each LAG were measured.

Age and growth rate estimation

Previous analyses validated annual LAG deposition in Kemp's ridley humerus bones (Snover and Hohn 2004; Avens et al. 2017), allowing for characterization of age at stranding through skeletochronology. Kemp's ridleys deposit a unique first-year growth mark, or "annulus," that differs from subsequent marks (Snover and Hohn 2004). For bones where the annulus was visible, an initial age estimate was

Table 1 Summary characteristics for Kemp's ridley sea turtles by stranding location

Location	Stranding data				Growth rate data	
	n^a	SCL (cm) Mean ± SD (range)	Estimated age (year) Mean ± SD (range)	Year range	*n*	Year range
wGoM	200	55.6 ± 10.9 (4.2–69.1)	11.87 ± 6.47 (0.00–30.25)	1997–2013	915	1988–2012
nGoM	439	40.0 ± 11.1 (16.6–66.2)	4.86 ± 4.37 (0.75–23.00)	1993–2016	1055	1990–2015
eGoM	142	41.1 ± 11.0 (20.3–65.4)	4.62 ± 3.23 (1.00–15.75)	1998–2013	354	1994–2013
sATL	362	38.2 ± 10.3 (19.3–66.7)	5.07 ± 3.23 (1.00–18.75)	1993–2016	1071	1990–2015
nATL	77	28.0 ± 4.1 (19.3–40.0)	3.67 ± 1.41 (1.00–8.50)	2001–2017	219	1996–2015

Western GoM (wGoM) = Texas; northern GoM (nGoM) = Louisiana, Mississippi, Alabama; eastern GoM (eGoM) = GoM coast of Florida); southern Atlantic (sATL) = Atlantic coast of Florida, Georgia, South Carolina, North Carolina, Virginia; northern Atlantic (nATL = Delaware, New Jersey, New York, Massachusetts). See Table S1 for state-specific data

[a] Stranding state unknown for 15 turtles (2 in Gulf of Mexico, 13 in Atlantic)

determined directly from LAG counts. However, bone resorption results in the loss of internal LAGs as sea turtles age (Zug et al. 1986), preventing the direct assessment of turtle age in larger individuals where the annulus has been resorbed. Therefore, for turtles where the annulus was not visible, a correction factor was developed based on the relationship between LAG numbers and diameters from known age individuals to estimate the number of LAGs lost to resorption for each bone (Parham and Zug 1997). An initial age estimate was then generated by adding the estimated number of resorbed LAGs to the number of visible LAGs. A final age estimate at stranding was made by adjusting initial age estimates to the nearest 0.25 years based on the mean hatch date for the population (June) and individual stranding date. Given that LAG deposition occurs in late winter/early spring and peak hatching for this species occurs during the summer (Snover and Hohn 2004), the first-year growth mark denotes an age of ~ 0.75 years, the next LAG an age of 1.75 years, and so on. Final age estimates were used to back-assign age estimates to individual LAGs. Similarly, a calendar year was back assigned to each LAG based on the date of stranding.

There is a strong allometric relationship between humerus section diameter (HSD) and SCL for Kemp's ridleys that allows for the back-calculation of body size estimates for measurable LAGs (Snover and Hohn 2004; Avens et al. 2017). We characterized the HSD:SCL relationship for newly processed turtle bones and combined that with the body proportional hypothesis back-calculation technique (BPH; Francis 1990) to estimate SCL for every measurable LAG, adjusted for turtle-specific SCL and HSD at death. Annual somatic growth rates were then calculated by taking the difference between SCL estimates of successive LAGs. In this way, multiple growth rate estimates were generated from each humerus bone (median 3 per turtle, range 1–8). Growth rate estimates were assigned to the calendar year associated with the LAG that begins each growth interval.

Environmental covariates

To investigate environmental drivers of sea turtle somatic growth variation, we evaluated the relative influence of the DWH oil spill, changing population density, and climate variability on Kemp's ridley somatic growth rates. While these stressors are not encompassing of all major environmental phenomena that may affect sea turtle growth rates, they were chosen for this analysis, because their potential influence matches the geographic scale encompassed by the somatic growth rate dataset.

The relationship between growth and population density was investigated using two population abundance metrics: (1) annual age class-specific abundance estimates obtained from the most recent Kemp's ridley population model used for status assessment (i.e., model-dependent metric; NMFS and USFWS 2015), and (2) cumulative annual hatchling production from the species' index nesting beach in Tamaulipas, Mexico, which comprises over 85% of nesting activity by the species (i.e., model-independent metric; data sourced from NMFS and USFWS 2015). This species is unique among sea turtles in that nearly its entire annual reproductive output is concentrated on only a handful of beaches in Mexico and South Texas that have been monitored and protected continuously since 1978. This has allowed for the near-complete census of nests laid and hatchlings produced from these beaches annually (NMFS and USFWS 2015). The population model used to derive age-specific abundance estimates is a deterministic age-based simulation model that uses known hatchling production since 1966 to predict the number of nests laid annually (NMFS and USFWS 2015). Model-derived abundance estimates by age class are only used through 2009 given uncertainties in the cause of post-2009 nest count fluctuations—mortality likely increased due to the DWH oil spill (Wallace et al. 2017), but other causes have also been proposed (Caillouet 2014; Caillouet et al. 2018; Kocmoud et al. 2019), creating substantial uncertainty in the underlying demographic processes for this species after 2009. Trends in population abundance metrics are summarized in Figure S1.

To elucidate potential relationships between changes in broad scale climate patterns and Kemp's ridley somatic growth variation, we considered three well-known modes of variability [North Atlantic Oscillation (NAO), Atlantic Multidecadal Oscillation (AMO), and the El Niño Southern Oscillation (ENSO)] that exert strong biophysical control on western North Atlantic Ocean ecosystems (Giannini et al. 2001; Greene et al. 2013; Karnauskas et al. 2015). Collectively, they influence ocean temperature, salinity, mixing, and circulation patterns that affect the productivity, distribution, growth, and survival of animals across all trophic levels (Drinkwater et al. 2003; Edwards et al. 2013; Karnauskas et al. 2015). For the NAO, we used the winter (December–March) NAO index (wNAO) given that the NAO is thought to exert the greatest influence on ocean ecosystems in the boreal winter (Drinkwater et al. 2003). For the ENSO, we used the Multivariate El Niño Southern Oscillation Index (MEI) Version 2, which integrates five meteorological variables: SST, surface air temperature, sea-level pressure, surface zonal winds, surface meridional winds, and Outgoing Longwave Radiation. Monthly AMO and bimonthly MEI data were obtained from NOAA's Earth System Research Laboratory (https://www.esrl.noaa.gov/psd/data/climateindices/), whereas wNAO data were obtained from the National Center for Atmospheric Research (https://climatedataguide.ucar.edu/climate–data/). Following Bjorndal et al. (2016, 2017), monthly AMO and bimonthly MEI data were averaged within a calendar year to create an annualized index used in all analyses.

Data analysis

We employed a suite of statistical tools to evaluate the independent and synergistic effects of the Deepwater Horizon oil spill, population density, and climate variability on Kemp's ridley growth rates. Given the retrospective nature of this study, the statistical approach taken was necessarily correlative and we, therefore, do not conclusively attribute causation. In most cases, analyses were restricted to juvenile growth data—binned by age class (age 0, 1, 2–5, 6–9) to increase statistical power—given that adult turtle growth rate data are poorly represented in the dataset. These age classes align with known ontogenetic differences in somatic growth rates and are similar to those used in age-structured population models (Snover et al. 2007; NMFS and USFWS 2015). Age 0 (ages 0–0.75) and 1 (ages 0.75–1.75) align with the oceanic life stage, but are separated here, because growth rates differ between these ages and a fraction of Kemp's ridleys begin to recruit to neritic habitats at age 1 (Avens et al. in review). All other age classes represent neritic life stages, i.e., small neritic juveniles (ages 2–5) and large neritic juveniles (age 6–9). As somatic growth rates differ between Kemp's ridleys that inhabit the U.S. Gulf of Mexico and Atlantic Coast (Avens et al. 2017; in review; this study), growth data were analyzed separately for turtles that stranded on beaches in these regions for all age classes but age 0—all age 0 turtles are assumed to occupy the same oceanic habitats in the central GoM.

To investigate DWH oil spill effects on somatic growth rates, we used two primary approaches: growth curve fits and temporal analysis. First, to examine population-level growth response, a family of von Bertalanffy growth functions (VBGFs) were fit to stranding size-at-age data for all turtles stranded before (1993–2009) and after (2011–2016) the DWH oil spill using non-linear least-squares regression. Eight models were considered to compare von Bertalanffy growth parameters (L_∞, asymptotic average length; K, Brody growth rate coefficient; t_0, age when the average length is zero) between both time periods that ranged from including identical parameter estimates for each time period (1 L_∞, 1 K, 1 t_0) to including fully unique parameter estimates for each time period (2 L_∞, 2 K, 2 t_0), and all model subsets in between (Table 2). Akaike information criterion (AIC) and Akaike weights (w_i) were used to evaluate and compare models (Burnham and Anderson 2002). In addition, given the non-independence of the full growth dataset, VBGFs were fit to measured SCL and estimated age at stranding only, eliminating SCL and age data estimated from growth marks. VBGFs were fit using data from GoM-stranded turtles only; large juvenile and adult Kemp's ridleys are rare along the U.S. Atlantic Coast and are thus underrepresented in our dataset, preventing the generation of robust Atlantic Kemp's ridley VBGFs. Growth functions were implemented using the FSA (Ogle et al. 2018) and nlstools (Baty et al. 2015) packages in R (version 3.5.3; R Core Team 2019).

Table 2 Summary statistics for the family of models used to evaluate whether von Bertalanffy growth parameter estimates (L_∞, K, t_0) differed for Kemp's ridley sea turtles stranded in the Gulf of Mexico before (1993–2009, $n = 402$) and after (2011–2016, $n = 362$) the Deepwater Horizon oil spill

Model	*df*	logLik	AIC	ΔAIC	W_i
Common L_∞ and $t_0 (K \neq K)$	5	–2201.34	4412.69	0.00	0.305
Common L_∞ $(K \neq K, t_0 \neq t_0)$	6	–2200.37	4412.74	0.05	0.298
Different L_∞, K, and t_0	7	–2199.91	4413.82	1.13	0.174
Common $t_0 (L_\infty \neq L_\infty, K \neq K)$	6	–2201.33	4414.67	1.98	0.113
Common K and t_0 $(L_\infty \neq L_\infty)$	5	–2202.91	4415.81	3.12	0.064
Common K $(L_\infty \neq L_\infty, t_0 \neq t_0)$	6	–2202.50	4416.99	4.3	0.036
Common L_∞ and K $(t_0 \neq t_0)$	5	–2204.76	4419.52	6.83	0.010
Common L_∞, K, and t_0	4	–2214.51	4437.02	24.33	0.000

L_∞ is the asymptotic average length, K is the Brody growth rate coefficient, and t_0 is the age when the average length is zero

We implemented two complementary techniques, regression coding schemes and cutpoint structural analyses, to quantitatively examine temporal changes in somatic growth rates. First, we used Reverse Helmert regression coding schemes to specifically compare growth rates in the years before (1995–2009) and after (2010–2015) the DWH oil spill. The advantage of this approach is that it allows for analysis of the entire growth dataset. We implemented coding schemes using age class-specific linear mixed-effects models that included annual growth rate as the dependent variable, year as the independent variable, and first-order autoregressive [AR(1)] covariance structure for growth increments within turtles. Turtle-specific random effects were also included to account for non-independence in the growth dataset—each turtle contributes multiple growth rates. We then used maximally selected rank statistics to identify the optimal cutpoint within each growth time series. This non-parametric approach was performed using the mean growth rates for each age class, is robust to small sample sizes (Hothorn and Lausen 2003; Müller and Hothorn 2004), and was implemented using the coin package in R (Zeileis et al. 2002; Hothorn et al. 2006).

Generalized additive models (GAMs) were used to examine relationships between population density metrics and mean age class-specific growth rates. Models included age-specific abundance (Abund) or cumulative hatchling production (HatchProd) as a fixed effect, an identity link, and a quasi-likelihood error function. Within each model, mean growth rates were weighted by sample size (i.e., number of growth rate estimates per year). For the oceanic life stages (age 0, age 1), age-specific growth rates were compared to the model-derived cumulative number of 0– and 1–year old turtles predicted to exist in a given year (metric 1) or the cumulative number of hatchlings produced in a given year and the year prior ($t_0 - t_{-1}$) (metric 2). For the neritic life stages (age 2–5, age 6–9), age-specific growth rates were compared to the model–derived cumulative number of juvenile turtles (ages 2–5) predicted to exist in a given year (metric 1) or the cumulative number of hatchlings produced 2–5 years in the past ($t_{-2} - \mathrm{t}_{-5}$) (metric 2). Models were implemented in R using the mgcv package (Wood 2006).

We used cross-correlation to examine relationships between mean age class-specific growth rates and climate indices. Following Bjorndal et al. (2016), GAMs with AR(1) covariance structure were fit to the annualized climate data to reveal underlying trends since 1950 for the wNAO and AMO and since 1979 for the MEI. Mean age class-specific growth rates were then compared to lagged (0–5 years) smoothing spline fits generated from the GAMs using the ccf function in R (version 3.5.3; R Core Team 2019). Cross-correlation coefficients were used to measure the degree of similarity between the two time series.

Finally, to directly compare the independent and synergistic effects of these environmental stressors on sea turtle growth rates, we performed an integrative analysis that incorporated the results of the aforementioned independent analyses into a family of GAMs for each age class. Models included various combinations of the three factors investigated as fixed effects, an identity link, and a quasi-likelihood error function. We weighted mean growth rates by sample size and used AIC and w_i to evaluate and compare models (Burnham and Anderson 2002).

Results

Age and growth

SCL and age at stranding ranged from 4.2 to 69.1 cm SCL and 0 to 30.25 years for turtles stranded on U.S. GoM beaches. Turtles stranded on U.S. Atlantic Coast beaches were 19.3–66.7 cm SCL and 1.00–18.75 years old (Tables 1, S1). Although their contribution to the breeding population is not well understood (NMFS and USFWS 2015), documentation of tagged Atlantic turtles nesting on the species' primary nesting beach in Mexico suggests that Atlantic Kemp's ridleys ultimately return to the GoM as large juveniles or maturing adults (Caillouet et al. 2015), resulting in relatively few adult animals on the Atlantic Coast. In total, skeletochronological analyses yielded 3647 annual growth rate estimates from 1235 turtles for the years 1988–2015 (Fig. 2). This constitutes the largest and most comprehensive dataset of Kemp's ridley somatic growth rates to date. Annual growth rates span ages 0 (first year of life) to 28.75, but data from younger ages (< 6 years) dominate the dataset (~ 75%), because younger/smaller turtles are the most abundant Kemp's ridley age classes in the population and thus constitute the majority of stranded turtles (Gallaway et al. 2016).

For both the GoM and Atlantic Coast, there were distinct spatiotemporal changes in humerus bone collection (Fig. 2).

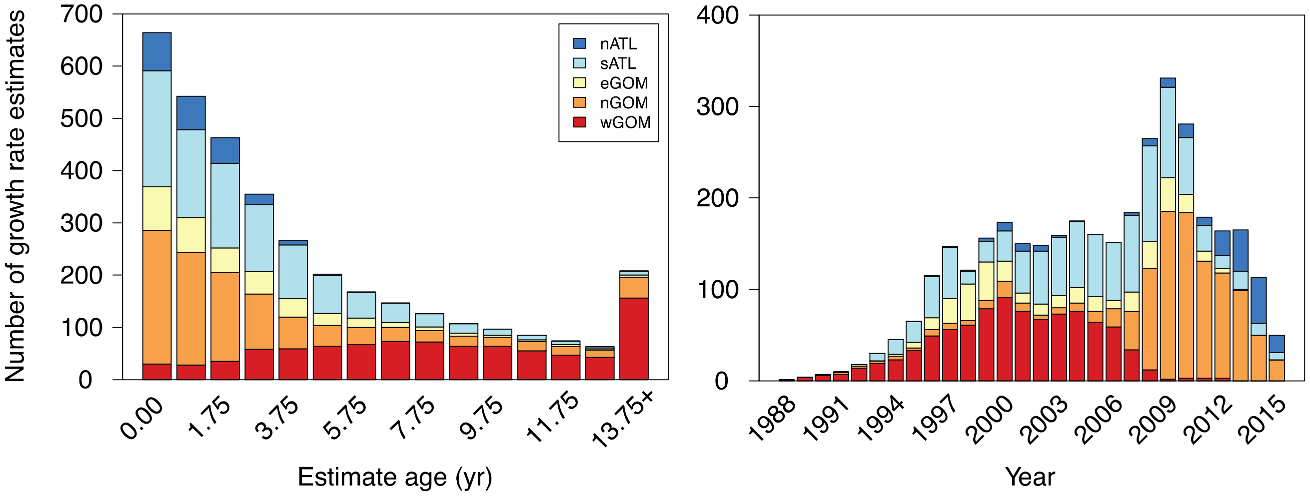

Fig. 2 Frequency histograms of Kemp's ridley sea turtle back-calculated somatic growth rates by stranding location, age, and year. *nATL* northern Atlantic (stranding location = Delaware, New Jersey, New York, Massachusetts), *sATL* southern Atlantic (stranding location = Atlantic coast of Florida, Georgia, South Carolina, North Carolina, Virginia), *eGoM* eastern Gulf of Mexico (stranding location = GoM coast of Florida), *nGoM* northern Gulf of Mexico (stranding location = Louisiana, Mississippi, Alabama), *wGoM* western Gulf of Mexico (stranding location = Texas)

Prior to 2010, GoM samples were primarily obtained from turtles stranded in Texas and Florida, whereas, after 2010, sample collection shifted to turtles stranded in Louisiana, Mississippi, and Alabama as part of the DWH oil spill response efforts. Along the U.S. Atlantic Coast, there was a similar shift in sample collection in 2014 and 2015 from turtles that stranded primarily in North Carolina and Virginia to turtles that stranded in Massachusetts. Using a general linear mixed model that accounted for year, age, AR(1) autocorrelation, and turtle-specific random effects, we found somatic growth rates did not differ within regions (Tukey's post hoc test1, $p > 0.05$), but were significantly lower in turtles from the Atlantic Coast (Tukey's post hoc test, $p < 0.05$). Examination of age class-specific growth rates indicates that these regional differences in growth manifest as early as age 1 and extend through the small neritic juvenile life stage (age 2–5) (Fig. 3). Regional differences in Kemp's ridley growth, size-at-age relationships, and maturation trajectories are further examined by Avens et al. (in review), whose analysis uses the same growth rate dataset presented herein.

The quantity of age class-specific somatic growth rate data was sparse for years preceding 1995, so all temporal growth analyses begin in 1995 and generally extend through 2014 or 2015 (Fig. 3). The datasets for age 0, age 2–5$_{\text{GoM}}$, age 2–5$_{\text{Atlantic}}$, and age 6–9$_{\text{GoM}}$ turtles are the largest and most continuous—all years have at least seven independent

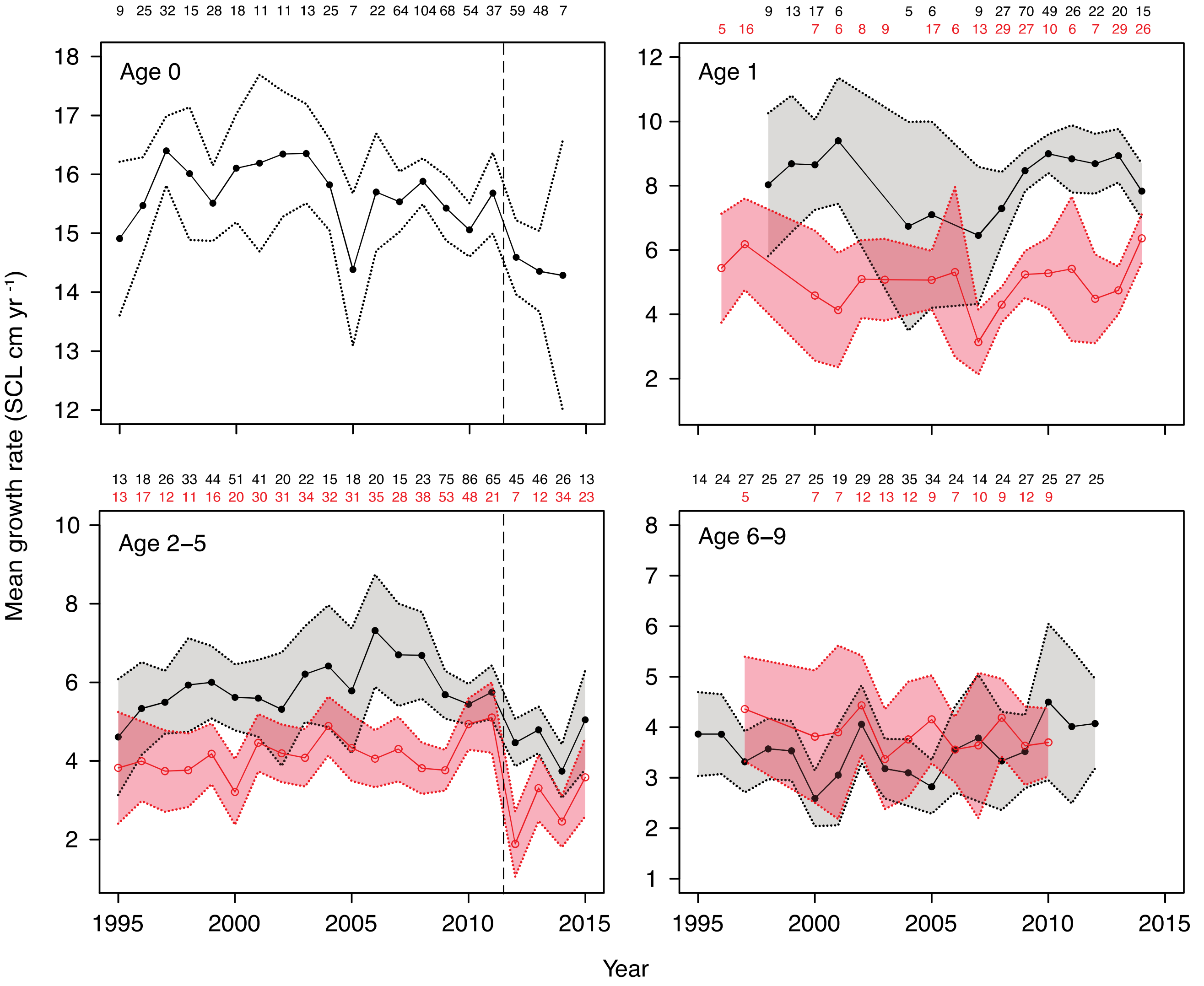

Fig. 3 Time series of mean Kemp's ridley sea turtle growth rate by age class. Dotted lines bound 95% confidence intervals. Age 0 includes data from both Gulf of Mexico (GoM) and Atlantic stranded turtles given that all Kemp's ridleys share oceanic habitats in the central GoM during the oceanic life stage. For all other age classes, GoM and Atlantic data were analyzed separately due to regional differences in growth rates (black shaded area = Gulf of Mexico stranded turtles; red shaded area = Atlantic stranded turtles). The number of growth observations are presented above each plot. Vertical dashed lines identify significant breaks in each time series where there was concordance among statistical methods evaluated (see Table 3). Data for years with $N < 3$ are excluded. *SCL* straightline carapace length

growth rate estimates (Fig. 3). In contrast, significant data gaps exist for age 1_{GoM}, age 1_{Atlantic}, and age 6–9_{Atlantic} turtles, and the datasets for age 6–9_{GoM} and age 6–9_{Atlantic} turtles only extend to 2012 and 2010, respectively. We, thus, urge caution when interpreting results from the age 1 and age 6–9 datasets given that they are discontinuous and do not reflect similar time frames as the data for ages 0 and 2–5.

Deepwater Horizon oil spill effects

The von Bertalanffy growth models fit to GoM turtle stranding length-at-age data suggested that somatic growth differed before and after the DWH oil spill (Table 2; Fig. 4). The model with the lowest AIC score and highest individual Akaike weight (w_i of 0.305) included common L_∞ and t_0 parameters but different K parameters for the two time periods (1993–2009 vs. 2011–2016; Table 2). Parameter estimates for the best model were $L_\infty = 65.04$, $t_0 = 1.52$, K (pre-DWH) = 0.192, and K (post-DWH) = 0.178. However, the next three best models had ΔAIC scores < 2.0 and w_i values between 0.113 and 0.298. While the parameters that differed or agreed between the two time periods varied in these models (common L_∞, different K and t_0; different L_∞, K, and t_0; common t_0, different L_∞ and K), all included two separate K parameters. The summed weights of the models that included separate K parameters for the two time periods was 0.890, indicating overall support for a growth rate reduction in the GoM after the DWH oil spill. Although we found some evidence for differences in K parameters, there was significant overlap in the distributions of the stranding length-at-age data before and after the DWH oil spill (Fig. 4), which suggests that this apparent difference may not be biologically meaningful or that there was not a systematic change in somatic growth across all U.S. GoM Kemp's ridley size classes. Insufficient length-at-age data for larger/older Atlantic Kemp's ridleys, which are thought to migrate back to the GoM prior to maturity (Caillouet et al. 2015), impeded our ability to fit von Bertalanffy growth models for these turtles (but see Avens et al. in review).

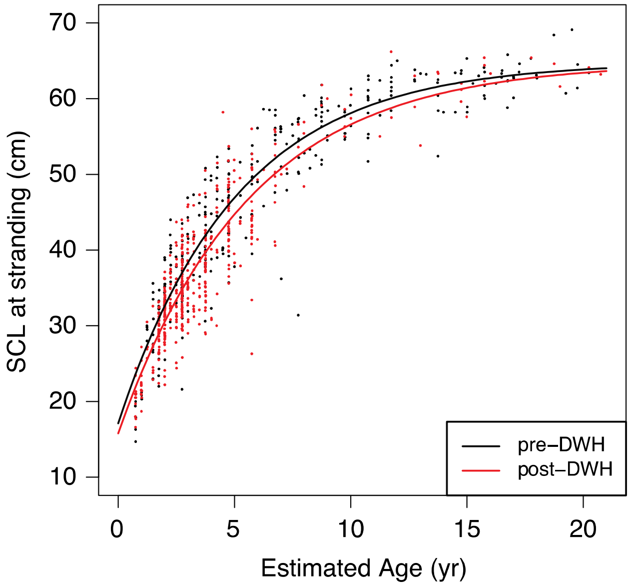

Fig. 4 Von Bertalanffy growth functions estimated for Kemp's ridley sea turtles stranded in the Gulf of Mexico before (1993–2009, $n = 402$) and after (2011–2016, $n = 362$) the Deepwater Horizon oil spill. VBGFs were based on measured straightline carapace length (SCL) and estimated age at stranding. Parameter estimates for the best model were $L_\infty = 65.04$, $t_0 = 1.52$, K (pre-DWH) = 0.192, and K (post-DWH) = 0.178

Reverse Helmert regression coding schemes applied to the full somatic growth dataset identified significant decreases in Kemp's ridley growth rates between 2011 and 2012 (Table 3). Relative to pre-DWH, growth rates in 2012 declined by 1–2 cm year^{-1} within the age 0 and age 2–5_{GoM} time series and greater than 3 cm year^{-1} within the age 2–5_{Atlantic} time series. Notably, this analysis revealed that growth rates in 2013 (age 0, age 2–5_{GoM}) and 2014 (age 2–5_{GoM}, age 2–5_{Atlantic}) were also significantly lower than pre-DWH growth rates. Relative to pre-DWH, growth rates from 2012 to 2015 were lower by 8.1% for age 0 turtles, 22.7% for age 2–5_{GoM} turtles, and 30.7% for age 2–5_{Atlantic}. Similar results were obtained using complementary cutpoint analyses, which identified significant decreases in mean annual somatic growth rates between 2011 and 2012 for turtles in the oceanic (age 0; max$T = 3.14$, $p = 0.005$) and small neritic juvenile life stages in both the U.S. GoM (age 2–5_{GoM}; max$T = 2.98$, $p = 0.008$) and Atlantic Coast (age 2–5_{Atlantic}; max$T = 3.37$, $p = 0.004$) (Table 3; Fig. 3). The cutpoint analysis did not identify any statistically significant changes in somatic growth rates for the age 1 and age 6–9 time series ($p < 0.05$), though regression coding identified a significant increase in age 1_{Atlantic} growth rates and decrease in age 6–9_{Atlantic} growth rates in 2014.

Taken together, these analyses provide evidence for a sharp decline in Kemp's ridley growth rates in the years following the DWH oil spill. However, the results of the temporal analyses did not align with our original hypotheses that predicted either an acute (H_{1A}) or chronic (H_{1B}) DWH oil spill impact on somatic growth rates beginning in 2010 for turtles in the GoM only (Fig. 1). Interestingly, this decline is evident, and proportionally greater, in Atlantic stranded turtles, which we predicted to exhibit no temporal changes in growth rates around the time of the DWH oil spill due to their spatial isolation. However, even with a decrease in growth rates, GoM small neritic juveniles (age 2–5) still grew faster than Atlantic conspecifics.

Table 3 Results of reverse Helmert regression coding schemes used to compare mean age class-specific growth rates of Kemp's ridley sea turtles before and after the Deepwater Horizon oil spill

Year comparison		Age class					
		Gulf of Mexico stranded turtles			Atlantic stranded turtles		
Comparison	0	1	2–5	6–9	1	2–5	6–9
2005 vs. 1995–2004				*			
2006 vs. 1995–2005			**				
2007 vs. 1995–2006					**		
2008 vs. 1995–2007							
2009 vs. 1995–2008							
2010 vs. 1995–2009						***	
2011 vs. 1995–2009						**	
2012 vs. 1995–2009	**		*			**	
2013 vs. 1995–2009	***		**				
2014 vs. 1995–2009			***		**	***	*
2015 vs. 1995–2009							–

Number of asterisks (*) indicates degree of significance based on p values (*$p < 0.05$, **$p < 0.01$, ***$p < 0.001$; empty cells mean no significant difference in mean growth rate). Colors indicate direction of change (black = increase, red = decrease). The complementary cutpoint analyses identified statistically significant structural shift in the age 0, age 2–5$_{\text{GoM}}$, and age 2–5$_{\text{Atlantic}}$ growth time series between 2011 and 2012. Years without data for comparison with pre-DWH growth rates are noted with a dash

Density-dependent effects

We found little support for density-dependent effects of cumulative turtle abundance and hatchling production on mean age class-specific somatic growth rates (Table S2). For all but age 2–5$_{\text{GoM}}$, GAMs revealed no significant relationship between these population density metrics and somatic growth ($p > 0.05$)—mean annual growth rates did not decline with increasing predicted juvenile abundance nor was there the presence of a threshold above which growth rates declined. The GAM response functions for both population abundance metrics and both GoM and Atlantic stranded turtles were generally similar (Figs. S2–S4).

Cumulative hatchling production was a significant ($p = 0.018$) predictor of age 2–5$_{\text{GoM}}$ somatic growth whereas cumulative age 2–5 abundance was only a marginally significant ($p = 0.051$) predictor (Table S2, Fig. 5). Growth rates at the highest age 2–5$_{\text{GoM}}$ population abundances were lower on average than those at lowest predicted population abundance, although 95% confidence intervals surrounding the annual means at the highest and lowest abundances overlapped extensively. Nevertheless, the shapes of this relationship for age 2–5$_{\text{GoM}}$ did align with our hypothesis related to density-dependent effects (H_2) on somatic growth rates (Fig. 1), which predicted a threshold above which growth rates begin to decline.

Climate effects

Mean annual growth rates tended to poorly correlate with the annualized climate indices with 0- to 5-year lags (Table S3). Cross correlations for most life stages (age 1, age 2–5, age 6–9) were generally negligible to weak (cross correlations ≤|0.40|), although cross correlations for age 6–9$_{\text{GoM}}$ with 4- and 5-year lags were –0.53 and –0.59 for wNAO and 0.52 and 0.60 for AMO. In contrast, mean annual growth rates exhibited moderate-to-strong correlations with all climate indices for the oceanic life stage (age 0; Fig. 6). The highest, consistent cross-correlation values for age 0 included a 2-year lag (wNAO = 0.59; AMO = –0.57; MEI = 0.60). Cross correlation values ≥|0.50| were also observed for the wNAO and AMO with 3- to 4-year lags, and the MEI with 0- to 1-year lags. The consistency in age class-specific growth patterns through time (Fig. 3) generally does not align with our predicted climate growth response (Fig. 1: H_3) of declining growth rates beginning in the late-1990s. However, our results suggest that climate variability may affect hatchling and oceanic juvenile growth during the oceanic life stage.

For the wNAO, positive cross correlations indicate that growth rates are higher when winter weather conditions in the western North Atlantic are warmer and wetter (Drinkwater et al. 2003) and during periods of high river discharge,

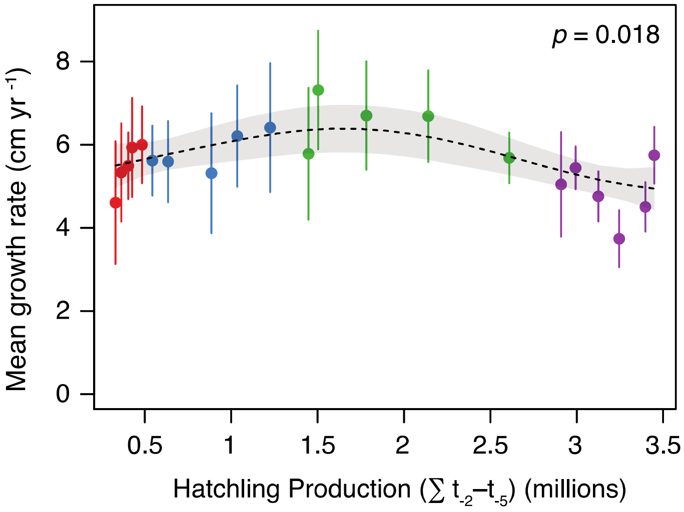

Fig. 5 Relationship between mean back-calculated growth rate and population density metrics for age 2–5 Kemp's ridley sea turtles stranded in the Gulf of Mexico. Dashed lines and gray ribbons are predicted values and 95% CI from GAM models with either cumulative hatchling production (left panel) or population abundance (right panel) included as a smoother term (see Table S2). Points are means ± 95% CI. *SCL* straightline carapace length. See Figs. S2–S4 for age 0, age 1, and age 6–9

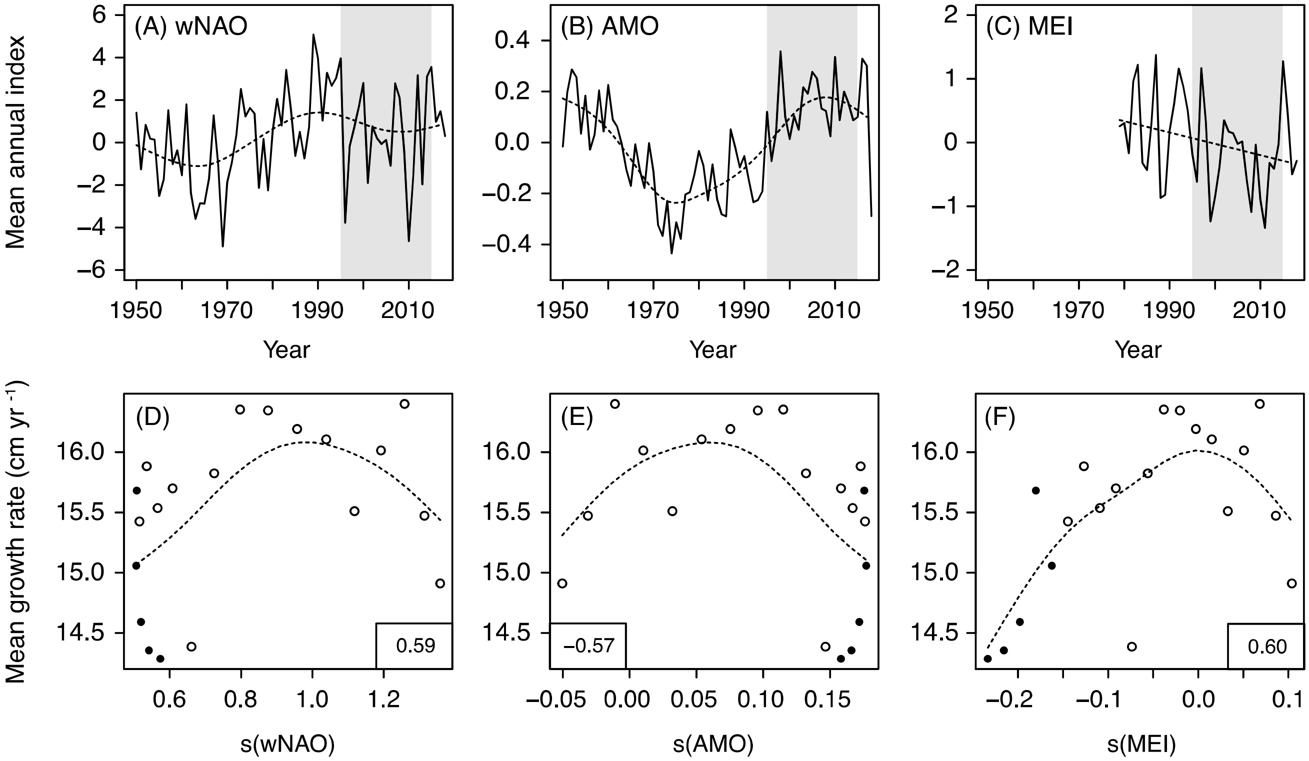

Fig. 6 Relationships between (**a**–**c**) climate indices and year and (**d**–**f**) mean age 0 growth rates and annualized climate indices (2-year lag). Dashed lines are the GAM trends. **a**–**c** Shaded area identifies study period. **d**–**f** Cross-correlation values are presented in boxes within each plot. Open circles are years 1995–2009, whereas filled circles are year 2010–2015. *wNAO* Winter North Atlantic Oscillation, *AMO* Atlantic Multidecadal Oscillation, *MEI* Multivariate El Niño Southern Oscillation Index

enhanced blue crab productivity, and reduced *Sargassum* abundance in the GoM (Sanchez-Rubio et al. 2011, 2018). Similar conditions along with cooler ocean temperatures are present during negative AMO phases (Karnauskas et al. 2015), which aligns with our observation of negative correlations between AMO and growth rates (i.e., positive wNAO and negative AMO are coupled). Positive correlations between the MEI and growth indicate that growth rates increase with increasing ocean temperatures (Giannini et al. 2001). However, our observation of declining oceanic stage turtle growth during a period of warming suggests that indirect negative effects of increasing ocean temperatures on sea turtle foraging habitat or prey may be negatively impacting their growth rates (Bjorndal et al. 2017).

Integrative effects

Three sets of GAMs were implemented to determine which environmental factors—either independently or synergistically—were most strongly related to age 0, age 2–5$_{\text{GoM}}$, and age 2–5$_{\text{Atlantic}}$ growth. Comparative models were restricted to these age classes, because they showed evidence of significant temporal, density, and climate effects within independent analyses. The three metrics evaluated in these models were (1) the temporal shift (TS) in growth observed in 2012, included as a categorical variable (TS$_{\text{pre}}$ = 1995–2011, TS$_{\text{post}}$ = 2012–2015); (2) cumulative hatchling production (HatchProd), included as a continuous variable; and, (3) the annualized GAM trend for the AMO index with a 2-year lag, included as a continuous variable. We generated models that included all combinations of these covariates as fixed effects, resulting in the evaluation of six models for each age class (i.e., TS + HatchProd + AMO, TS + HatchProd, TS + AMO, TS, HatchProd, AMO). The HatchProd and AMO covariates displayed a moderate-to-high degree of collinearity with variance inflation factors of ~ 6 and correlation coefficients between 0.83 and 0.92, indicating that the coefficients in the global model (TS + HatchProd + AMO) may be poorly estimated and that the p values may be questionable (Dormann et al. 2012). We include the model herein for comparison but urge caution when interpreting the results.

Within each age class, multiple models had ΔAIC scores less than two and were thus considered strong potential predictors of mean age class-specific growth rates (Table 4). In all cases, these top models included TS alone or in combination with HatchProd and AMO. However, in most cases, HatchProd and AMO were not statistically significant predictor variables (Table 5). The HatchProd and AMO only models explained the least variation in somatic growth for all age classes.

For age 0, the top model included TS and HatchProd as fixed effects based on AIC score and Akaike weight. However, the next three best models were within 2 AIC, which included TS + HatchProd, TS only, or TS + HatchProd + AMO as fixed effects. The cumulative Akaike weight for these top four models was 1.00 and TS was the only statistically significant predictor of mean age 0 growth rates in these models (Table 5).

Table 4 Summary statistics for the family of generalized additive models used to evaluate the influence of covariates [temporal shift (TS), hatchling production (HatchProd), and Atlantic Multidecadal Oscillation (AMO)] on mean age class-specific growth rates for age 0 and age 2–5 Kemp's ridley sea turtles

Model	*df*	logLik	AIC	ΔAIC	W_i
(a) Age 0					
TS + HatchProd	4.00	−11.28	30.57	0.00	0.32
TS + AMO	5.34	−10.04	30.76	0.19	0.29
TS	3.00	−12.57	31.15	0.58	0.24
TS + AMO + HatchProd	5.00	−11.02	32.05	1.48	0.15
HatchProd	3.00	−20.72	47.45	16.88	0.00
AMO	3.39	−20.69	48.15	17.58	0.00
(b) Age 2–5, Gulf of Mexico					
TS + AMO + HatchProd	5.00	−11.17	32.35	0.00	0.49
TS + HatchProd	6.74	−9.58	32.64	0.29	0.43
TS	3.00	−15.51	37.03	4.68	0.05
TS + AMO	4.00	−14.85	37.71	5.36	0.03
HatchProd	5.46	−16.45	43.83	11.48	0.00
AMO	3.00	−23.51	53.02	20.67	0.00
(c) Age 2–5, Atlantic					
TS	3.00	−14.86	35.72	0.00	0.45
TS + HatchProd	4.00	−14.48	36.95	1.23	0.24
TS + AMO	4.00	−14.83	37.65	1.93	0.17
TS + AMO + HatchProd	5.00	−14.09	38.17	2.45	0.13
HatchProd	3.00	−21.41	48.82	13.10	0.00
AMO	3.00	−21.98	49.97	14.25	0.00

TS is a factor with categorization based on breakpoint identified in temporal analyses (pre-shift = 1995–2011, post-shift = 2012–2015). HatchProd is cumulative hatchling production for years, $t(x)$, prior to a given year (age $0 = \Sigma t_0 - t_{-1}$, age $2\text{–}5 = \Sigma t_{-2} - t_{-5}$). AMO is the annualized GAM trend for the index with a 2-year lag

For age 2–5$_{\text{GoM}}$, the best model included all three covariates as fixed effects and had an Akaike weight of 0.49. Notably, all three covariates were statistically significant predictors of age 2–5$_{\text{GoM}}$ somatic growth rates within this top model. A second model, TS + HatchProd, was within 0.29 AIC of this best model. Only TS was a statistically significant predictor of mean age 2–5$_{\text{GoM}}$ growth rates in this second model (Table 5), although HatchProd was marginally significant ($p = 0.072$). The cumulative Akaike weight of these top two models was 0.92.

For age 2–5$_{\text{Atlantic}}$, the top model included TS only and had an Akaike weight of 0.45. Two additional models had ΔAIC scores less than two (TS + HatchProd and TS + AMO), providing for a cumulative Akaike weight of 0.86 for the top three models. As for the age 0 models, TS was the only statistically significant predictor of mean age 2–5$_{\text{Atlantic}}$ growth rates within the top age 2–5$_{\text{Atlantic}}$ models (Table 5).

Table 5 Summary of statistical output for generalized additive models (GAMs) used to evaluate the influence of potential environmental covariates [temporal shift (TS), hatchling production (HatchProd), and Atlantic Multidecadal Oscillation (AMO)] on mean age class-specific growth rates for age 0 and age 2–5 Kemp's ridley sea turtles

Model	Dev (%)	Adj. R^2	Smooth terms				Parametric coefficients				
			Var	Edf	F	Prob(F)	Var	Est	SE	t	Pr > |t|
(a) Age 0 ($n = 21$ years)											
$\text{GAM}_{\text{TS + HatchProd}}$*	65.1	0.61	HatchProd	1.00	2.35	0.142	TS_{pre}	1.13	0.22	5.12	**< 0.001**
$\text{GAM}_{\text{TS + AMO}}$*	69.0	0.64	AMO	1.90	2.34	0.235	TS_{pre}	1.13	0.22	5.26	**< 0.001**
GAM_{TS}*	60.6	0.59	–	–	–	–	TS_{pre}	1.20	0.22	5.40	**< 0.001**
$\text{GAM}_{\text{TS + AMO + HatchProd}}$*	66.0	0.60	AMO HatchProd	1.00 1.00	0.43 1.30	0.522 0.270	TS_{pre}	1.15	0.23	5.08	**< 0.001**
$\text{GAM}_{\text{HatchProd}}$	14.3	0.10	HatchProd	1.00	3.18	0.091	–	–	–	–	–
GAM_{AMO}	14.6	0.09	AMO	1.21	1.68	0.165	–	–	–	–	–
(b) Age 2–5, Gulf of Mexico ($n = 21$ years)											
$\text{GAM}_{\text{TS + AMO + HatchProd}}$*	69.2	0.64	AMO HatchProd	1.00 1.00	8.69 7.14	**0.009** **0.016**	TS_{pre}	0.99	0.29	3.38	**0.004**
$\text{GAM}_{\text{TS + HatchProd}}$*	73.6	0.67	HatchProd	3.07	2.53	0.072	TS_{pre}	1.07	0.28	3.84	**0.001**
GAM_{TS}	53.5	0.51	–	–	–	–	TS_{pre}	1.29	0.28	4.67	**< 0.001**
$\text{GAM}_{\text{TS + AMO}}$	56.3	0.52	AMO	1.00	1.17	0.294	TS_{pre}	1.39	0.29	4.80	**< 0.001**
$\text{GAM}_{\text{HatchProd}}$	49.1	0.41	HatchProd	2.84	4.11	**0.018**	–	–	–	–	–
GAM_{AMO}	0.4	–0.05	AMO	1.00	0.07	0.793	–	–	–	–	–
(c) Age 2–5, Atlantic ($n = 21$ years)											
GAM_{TS}*	50.0	0.47	–	–	–	–	TS_{pre}	1.39	0.32	4.36	**< 0.001**
$\text{GAM}_{\text{TS + HatchProd}}$*	51.8	0.46	HatchProd	1.00	0.68	0.422	TS_{pre}	1.55	0.38	4.10	**< 0.001**
$\text{GAM}_{\text{TS + AMO}}$*	50.1	0.45	AMO	1.00	0.06	0.808	TS_{pre}	1.40	0.34	4.19	**< 0.001**
$\text{GAM}_{\text{TS + AMO + HatchProd}}$	53.5	0.45	AMO HatchProd	1.00 1.00	0.64 1.24	0.433 0.280	TS_{pre}	1.69	0.42	4.03	**< 0.001**
$\text{GAM}_{\text{HatchProd}}$	6.7	0.02	HatchProd	1.00	1.36	0.257	–	–	–	–	–
GAM_{AMO}	1.4	–0.04	AMO	1.00	0.27	0.604	–	–	–	–	–

TS is a factor with categorization based on breakpoint identified in temporal analyses ($\text{TS}_{\text{pre}} = 1995–2011$, $\text{TS}_{\text{post}} = 2012–2015$). HatchProd is cumulative hatchling production for years, $t(x)$, prior to a given year (age $0 = \Sigma t_0 - t_{-1}$, age $2–5 = \Sigma t_{-2} - t_{-5}$). The models are ordered as in Table 4, with age class-specific models with ΔAIC scores < 2 denoted with an asterisk (*). Bold values denote statistically significant covariates ($p < 0.05$)

AMO annualized GAM trend for the index with a 2-year lag, *Dev* deviance explained by the model, *Edf* estimated degrees of freedom

Discussion

Marine ecosystems are experiencing unprecedented change due to the combined effect of suites of environmental factors. As population responses to ecosystem change are manifested through changes in animal demographic rates, establishing mechanistic links between environmental stressors and demographic variation is fundamental to understanding and predicting species population dynamics. Through an analysis of 20+ years of somatic growth rate data, we show that juvenile Kemp's ridley sea turtles experienced a significant, multi-year reduction in somatic growth from 2012 to 2015 that spanned multiple life stages (oceanic and small neritic juveniles) and habitats (GoM and U.S Atlantic). Specific mechanisms underpinning this population-wide temporal shift in growth remain elusive, but likely include direct and indirect negative effects of the DWH oil spill. Among the environmental factors investigated, drivers of the 2012 change in growth constitute the greatest contributor to Kemp's ridley somatic growth variation in recent decades. However, our integrative analysis indicated that regional climate variability and changing population density have likely had synergistic effects on oceanic (climate only) and small neritic (climate + population density) juvenile growth rates in the GoM. Our results contrast with other post-DWH oil spill studies that observed immediate effects on growth rates in invertebrates and fish in 2010, but align with observations of declining stranded turtle nutritional condition in the northern GoM beginning in 2012 (Stacy 2015), a phenomena of unknown origin but that would likely reduce growth rates.

Growth and the Deepwater Horizon oil spill

We hypothesize that the 2012 reductions in growth observed across the species' U.S. range result partially from indirect negative effects of the DWH oil spill on sea turtle health mediated by changes in the food web. We initially predicted a direct DWH-associated growth response would manifest in 2010 for GoM turtle life stages only given the coincidence of the oil spill and annual initiation of sea turtle somatic growth, and the observation of immediate changes in other species' demographic rates (e.g., Rozas et al. 2014; Brown-Peterson et al. 2016; Herdter et al. 2017; Perez et al. 2017). However, the lack of a growth response in 2010 suggests that the DWH oil spill may not have had immediate, direct impacts on sea turtle growth rates. Still, indirect negative effects are likely given the scale of the oil spill, whose impact may have taken years to transcend food webs to influence sea turtle demographic rates.

Chronic exposure to DWH-associated environmental toxins may threaten the long-term health of marine megafauna in the GoM, including sea turtles. Following the 1989 Exxon Valdez oil spill, chronic exposure to weathered oil entrained in sediments delayed the recovery of a wide range of taxa for decades due to long-term effects on species demographic rates (Peterson et al. 2003). Similar effects appear to be compromising the long-term health, reproductive success, and survival of GoM bottlenose dolphins (Schwacke et al. 2014, 2017; Lane et al. 2015; Kellar et al. 2017). Much like other mobile marine predators, sea turtles were exposed to DWH-associated environmental toxins for years following the oil spill due to its spatial overlap with key oceanic and neritic foraging grounds that they continued to use (Shaver et al. 2013; Hart et al. 2014; Wallace et al. 2017; Berenshtein et al. 2020). The leaching and resuspension of oil-contaminated sediments represents a continued, long-term threat to coastal GoM food webs (Murawski et al. 2016; Rouhani et al. 2017; Romero et al. 2017). Additionally, both oceanic and neritic sea turtles directly ingested spilled oil and absorbed polycyclic aromatic hydrocarbons (PAHs) into their tissues (Ylitalo et al. 2017; Reich et al. 2017), which can cause adverse physiological effects in animals such as reduced growth (e.g., Meador et al. 2006; Albers 2006).

Interestingly, the observed 2012 decline in somatic growth aligns with a simultaneous deterioration of neritic stranded turtle nutritional condition and shift in sea turtle foraging behavior in the northern GoM. Necropsies of juvenile Kemp's ridleys (25–60 cm SCL, ~ 2–9 years) stranded in the northern GoM between 2010 and 2014 revealed significant reductions in the size of turtle fat stores beginning in 2012 (Stacy 2015). Coincident with this change was a substantial increase in Kemp's ridley incidental captures at fishing piers in Mississippi where turtles regularly attempted to eat fishing bait (Coleman et al. 2016). Rudloe and Rudloe (2005) previously linked this behavior to reduced growth rates in Kemp's ridleys. The integration of these findings with those herein suggest a fundamental shift in the functioning of northern GoM food webs prior to 2012 that impacted turtle foraging, nutritional condition, and growth. Causal factors for changes in nutritional condition and foraging behaviors have not been identified, but the spatiotemporal proximity to the DWH oil spill is conspicuous. Alternatively, these changes may relate to the collapse of the Mississippi blue crab fishery in 2011, which has been attributed to freshwater inundation from the opening of the Bonnet Carré Spillway (GSMFC 2015), and may also be connected to negative effects of the DWH oil spill (Alloy et al. 2015; Giltz and Taylor 2017). Comparisons of the nutritional status and growth histories of dead stranded turtles may improve our understanding of temporal variability in Kemp's ridley growth dynamics.

Negative impacts of the DWH oil spill on oceanic habitats were severe and were predicted to also impact the growth rates of oceanic stage turtles beginning in 2010. However, much like the GoM small neritic juvenile life stage, we did not observe a significant decline in oceanic stage turtle growth rates in 2010 but in 2012. All Kemp's ridleys associate with floating *Sargassum* in GoM oceanic habitats for the first 1–3 years of life before recruiting to neritic habitats along either the GoM or U.S. Atlantic Coast (TEWG 2000; Avens et al. in review). Following the oil spill, *Sargassum* tended to accumulate oil, become hypoxic, and sink (Powers et al. 2013). The loss or compromise of this critical habitat would have ultimately increased predation rates and foraging costs, and reduced prey availability (Witherington 2002). Given the vulnerability of oceanic stage turtles, the lack of a 2010 and 2011 growth response may indicate stronger initial DWH effects on survival rather than growth (McDonald et al. 2017). Interestingly, *Sargassum* abundance was anomalously high in 2011 and 2012 throughout the tropical North Atlantic, which should have renewed these habitats and provided oceanic stage turtles with optimal conditions for growth and survival (Witherington et al. 2012; Gower et al. 2013; Powers et al. 2013). That growth rates instead declined in 2012 and 2013 suggests either lingering effects of the DWH oil spill on these food webs or the influence of another environmental stressor (outlined below).

The observation of a strong, proportionally greater decline in Atlantic small neritic juvenile growth in 2012 was unexpected given our initial assumption that Atlantic Kemp's ridley growth rates would not change following the DWH oil spill. The causal factors for this decline remain unknown, but could be related to negative effects of the DWH oil spill on GoM *Sargassum* habitats. It is well established that early nutrition can impact life-time growth through 'silver spoon' effects (Larsson and Forslund 1991; Madsen and Shine 2000; McAdam and Boutin

2003; Gaillard et al. 2003), and many of the Atlantic Kemp's ridleys that exhibited reduced growth in 2012–2015 would have occupied GoM *Sargassum* habitats in 2010 during their oceanic life stage. Therefore, it is plausible that cumulative impacts of the DWH oil spill on oceanic turtle habitats and physiology compromised their long-term health and were carried with them into non-impacted marine habitats both within and outside the GoM (Putman et al. 2015). We still do not understand why Atlantic Kemp's ridleys grow more slowly than their GoM counterparts (reviewed in Avens et al. 2017, in review), but the underlying cause could have interacted with carryover effects of the DWH oil to amplify their cumulative growth response and cause the proportionally greater decline in Atlantic Kemp's ridley growth rates. Improved understanding of drivers of Atlantic Kemp's ridley growth variation will be key to disentangling potential effects of the DWH oil spill.

Interactive effects of multiple environmental stressors

We found support for additive or synergistic effects of changing population density and climate variability on GoM turtle growth rates in addition to the post-2012 shift in growth. Our integrative analysis identified all three environmental factors examined as significant predictors of GoM small neritic juvenile somatic growth. One hypothesis for the recent fluctuations in Kemp's ridley nest counts after a period of exponential growth is that the carrying capacity of the GoM has been reached for this species (Gallaway et al. 2016; Caillouet et al. 2016, 2018). Empirical support for this hypothesis, however, has been lacking due to insufficient data independent of the species' nesting trends (but see Shaver et al. 2016), which are confounded after 2010 with unknown effects of the DWH oil spill. Within both independent and integrative analyses, we found strong support for a statistically significant relationship between population density metrics and GoM small neritic juvenile growth. Specifically, we observed lower, more variable growth rates at the highest population densities and a multi-year declining growth trend that began in the mid-2000s, which generally aligns with our initial predictions and observations in Avens et al. (2017). However, these findings are equivocal. Growth rates at the highest population densities (2010–2015) overlap considerably with growth rates at the lowest population densities examined (1995–1999; Fig. 5). Therefore, more research is needed, especially extensions of the skeletochronology dataset, before we can confidently assert Kemp's ridley population density is influencing their somatic growth rates. Importantly, our findings contrast with those that have suggested that density-dependent processes have influenced this population as early as the year 2000 (Caillouet et al. 2018; Caillouet 2019).

Climate variability may also influence both oceanic and small neritic juvenile Kemp's ridley growth rates in the GoM, though our independent and integrative analyses provided conflicting results. Recent studies have linked decades-long declines in sea turtle growth rates in the Caribbean Basin to a late-1990s climate-driven ecological regime shift (Bjorndal et al. 2013, 2016, 2017). Herein, cross correlations between lagged climate indices and somatic growth rates identified moderate-to-strong correlations for oceanic stage turtles, but climate was not a significant predictor within the integrative analysis. The opposite pattern was observed for GoM small neritic juveniles, where the climate indices were poorly correlated with somatic growth within the independent analysis, but identified as a significant predictor in the top integrative model. Conflicting results for small neritic juveniles may be due in part to issues with collinearity between population density and climate metrics in the top integrative model which could inflate variance in model parameters for one or both variables (Dormann et al. 2012). These issues aside, as ectotherms, sea turtle growth rates would generally be expected to correlate with temperature-driven climate indices such as the AMO and MEI, particularly during the oceanic stage when they occupy epipelagic habitats and have limited capacity to fight ocean currents. Therefore, changes in growth rates for oceanic stage turtles may reflect the synergistic effects of regional climate variability on oceanic habitats and lingering impacts of the DWH oil spill, whereas changes in growth rates for GoM small neritic juveniles may be more strongly influenced by interactive effects of the DWH oil spill and population density.

Our analysis focused on three environmental stressors with wide-reaching influence, but many other environmental factors likely contributed to Kemp's somatic variation during the study period, particularly for U.S. Atlantic turtles. Anomalous heatwaves occurred in the western North Atlantic in 2012 and 2016 that caused widespread ecosystem change, including shifts in species distributions and recruitment (Mills et al. 2013; Pershing et al. 2015, 2018; Henderson et al. 2017). Though effects of these heatwaves on sea turtles remain unknown, negative effects of rising temperatures on Kemp's ridley foraging habitats and prey could have indirectly impacted their growth rates, a mechanism suggested to explain the declining growth trends in western North Atlantic loggerhead, green, and hawksbill sea turtles in recent decades (Bjorndal et al. 2016, 2017). More broadly, local water temperatures hold the potential to substantially contribute to somatic growth variation in this species given that its geographic distribution spans > 20° latitude (18°N to 43°N) and that parts of the U.S. Atlantic Coast are warming faster than anywhere else in the world (Pershing et al. 2015). Establishing mechanistic links between sea turtle growth rates and local water temperatures, such as through comparison of terminal humerus bone growth rates with local temperature records, will be critical to understanding how sea turtles may respond to climate change (Stubbs et al. 2020). A suite of other environmental factors—regional diet variation, prey availability and distribution, intra-and interspecific competition, genetics, and migration distance (see Avens et al. 2017, in review; Ramirez et al. 2020)—have also been identified as possible contributors to Kemp's ridley somatic growth variation and warrant further study.

Implications of reduced somatic growth rates

Whether the observed growth declines represent a biologically meaningful change requires further evaluation. Somatic growth and body size influence a host of other demographic processes, such as mortality rate, time to maturity, and fecundity, that cumulatively impact individual fitness and species population dynamics (Madsen and Shine 2000; Dmitriew 2011). Therefore, any alteration to an individual's growth trajectory has the potential to have cascading effects on population demography. The growth rate declines which we observed are well within the natural variation for this species (reviewed in Avens et al. 2017), but their severity varied by life stage. For example, oceanic stage turtle growth rates declined by ~ 8% after 2012, but GoM and Atlantic small neritic juvenile growth rates declined by ~ 20% and ~ 30%, respectively. Avens et al. (in review) determined that the U.S. GoM vs. Atlantic Coast differences in somatic growth may delay Atlantic Kemp's ridley maturity by 2–3 years relative to GoM counterparts. Herein, post-2012 GoM Kemp's ridley growth rates are similar to those of pre-2012 Atlantic Kemp's ridleys, which suggests that a multi-year delay in maturation for GoM turtles is possible. Moreover, the proportionally greater decline in Atlantic Kemp's ridley growth rates may further deepen their life-long disadvantage relative to GoM conspecifics. Integration of somatic growth data into demographic models may shed important light on the impacts of these growth changes on sea turtle population dynamics and implications for conservation and management.

Conclusion

Through analyses of 20+ years of dead stranded turtle humeri, we examined the somatic growth response of the critically endangered Kemp's ridley sea turtle to multiple environmental factors. We identified a simultaneous decrease in growth rates beginning in 2012 for oceanic and small neritic juveniles that stranded in U.S. waters. We hypothesize that these changes are due in part to deleterious effects of the DWH oil spill on sea turtles and their GoM habitats. For certain life stages, this growth response may reflect synergistic effects of the DWH oil spill, climate variability, and density-dependent processes. Our understanding of the links between the DWH oil spill and sea turtle growth rates would be greatly enhanced through geochemical analyses (e.g., PAHs, trace elements, and isotopes) of turtle bone tissues, which may reveal direct evidence of exposure to DWH-associated environmental toxins (e.g., Wise et al. 2014; Wilson et al. 2015; López-Duarte et al. 2016; Romero et al. 2018). This study highlights the critical importance of long-term, continuous collection of sea turtle humerus bones for status and threat assessment. To date, the collection of dead stranded turtle humeri has been inconsistent across both space and time, and we lack any knowledge of growth rates of Kemp's ridleys within Mexican waters, where some Kemp's ridleys turtles forage. Within the U.S., widespread collection of Kemp's ridley bones ended in 2015, but resumption of these efforts and initiation of bone collection in Mexico will be necessary to fully evaluate the long-term influence of these and other environmental factors on sea turtle growth rates.

Acknowledgements We thank the hundreds of federal, state, and private partners that collectively form the Sea Turtle Stranding and Salvage Network for their invaluable work without which this study would not have been possible. We also thank K. Magnusson for providing lab space and equipment for skeletochronological analysis, the Oregon State University Linus Pauling Institute for use of their imaging systems, and B. Stacy and J. Keene (NOAA) for collection of humeri associated with the DWH Natural Resource Damage Assessment. Thank you to J. Cordeiro, M. Davis, H. Hagler, and M. VanBemmel for assistance with laboratory analyses. Thank you also to J. Miller, A. Shiel, J. McKay, and two anonymous reviewers for comments on this manuscript. Funding for M. Ramirez and this project were provided by the NSF Graduate Research Fellowship Program. The contents of this publication are solely the responsibility of the authors and do not necessarily represent the official views of the U.S. Department of Commerce, National Oceanic and Atmospheric Administration. Research was conducted under USFWS permit number TE-676379-5 issued to the NMFS Southeast Fisheries Science Center.

Compliance with ethical standards

Conflict of interest The authors declare they have no conflict of interest.

Ethical approval This article does not contain any studies with human participants or live animals performed by any of the authors.

Data availability The dataset generated and analyzed in the current study are available from the corresponding author upon reasonable request.

References

Albers PH (2006) Birds and polycyclic aromatic hydrocarbons. Avian Poult Biol Rev 17:125–140. https://doi.org/10.3184/147020606783438740

Alloy MM, Boube I, Griffitt RJ, Oris JT, Roberts AP (2015) Photo-induced toxicity of Deepwater Horizon slick oil to blue crab

(*Callinectes sapidus*) larvae. Environ Toxicol Chem 34(9):2061–2066. https://doi.org/10.1002/etc.3026

Avens L, Snover ML (2013) Age and age estimation in sea turtles. In: Wyneken J, Lohmann KJ, Musick JA (eds) The biology of sea turtles. CRC Press, Boca Raton, pp 97–134

Avens L, Goshe LR, Coggins L, Shaver DJ, Higgins B, Landry AM, Bailey R (2017) Variability in age and size at maturation, reproductive longevity, and long-term growth dynamics for Kemp's ridley sea turtles in the Gulf of Mexico. PLoS ONE 12:e0173999. https://doi.org/10.1371/journal.pone.0173999

Avens L, Ramirez MD, Hall AG, Snover ML, Haas HL, Godfrey MH, Goshe LR, Cook M, Heppell SS (in review) Regional differences in Kemp's ridley sea turtle growth trajectories and expected age at maturation. Mar Ecol Prog Ser

Baty F, Ritz C, Charles S, Brutsche M, Flandrois J-P, Delignette-Muller M-L (2015) A toolbox for nonlinear regression in *R*: the package nlstools. J Stat Softw. https://doi.org/10.18637/jss.v066.i05

Beaugrand G, McQuatters-Gollop A, Edwards M, Goberville E (2013) Long-term responses of North Atlantic calcifying plankton to climate change. Nat Clim Change 3:263–267. https://doi.org/10.1038/nclimate1753

Berenshtein I, Paris CB, Perlin N, Alloy MM, Joye SB, Murawski S (2020) Invisible oil beyond the Deepwater Horizon satellite footprint. Sci Adv 6:eaaw8863. https://doi.org/10.1126/sciadv.aaw8863

Bevan E, Wibbels T, Najera BMZ, Sarti L, Martinez FI, Cuevas JM, Gallaway BJ, Pena LJ, Burchfield PM (2016) Estimating the historic size and current status of the Kemp's ridley sea turtle (*Lepidochelys kempii*) population. Ecosphere 7:e01244. https://doi.org/10.1002/ecs2.1244

Beyer J, Trannum HC, Bakke T, Hodson PV, Collier TK (2016) Environmental effects of the Deepwater Horizon oil spill: a review. Mar Pollut Bull 110:28–51. https://doi.org/10.1016/j.marpolbul.2016.06.027

Bjorndal KA, Schroeder BA, Foley AM, Witherington BE, Bresette M, Clark D, Herren RM, Arendt MD, Schmid JR, Meylan AB, Meylan PA, Provancha JA, Hart KM, Lamont MM, Carthy RR, Bolten AB (2013) Temporal, spatial, and body size effects on growth rates of loggerhead sea turtles (*Caretta caretta*) in the Northwest Atlantic. Mar Biol 160:2711–2721. https://doi.org/10.1007/s00227-013-2264-y

Bjorndal KA, Chaloupka M, Saba VS, Diez CE, van Dam RP, Krueger BH, Horrocks JA, Santos AJB, Bellini C, Marcovaldi MAG, Nava M, Willis S, Godley BJ, Gore S, Hawkes LA, McGowan A, Witt MJ, Stringell TB, Sanghera A, Richardson PB, Broderick AC, Phillips Q, Calosso MC, Claydon JAB, Blumenthal J, Moncada F, Nodarse G, Medina Y, Dunbar SG, Wood LD, Lagueux CJ, Campbell CL, Meylan AB, Meylan PA, Burns Perez VR, Coleman RA, Strindberg S, Guzmán-H V, Hart KM, Cherkiss MS, Hillis-Starr Z, Lundgren IF, Boulon RH, Connett S, Outerbridge ME, Bolten AB (2016) Somatic growth dynamics of West Atlantic hawksbill sea turtles: a spatio-temporal perspective. Ecosphere 7:e01279. https://doi.org/10.1002/ecs2.1279

Bjorndal KA, Bolten AB, Chaloupka M, Saba VS, Bellini C, Marcovaldi MAG, Santos AJB, Bortolon LFW, Meylan AB, Meylan PA, Gray J, Hardy R, Brost B, Bresette M, Gorham JC, Connett S, Crouchley BVS, Dawson M, Hayes D, Diez CE, van Dam RP, Willis S, Nava M, Hart KM, Cherkiss MS, Crowder AG, Pollock C, Hillis-Starr Z, Muñoz Tenería FA, Herrera-Pavón R, Labrada-Martagón V, Lorences A, Negrete-Philippe A, Lamont MM, Foley AM, Bailey R, Carthy RR, Scarpino R, McMichael E, Provancha JA, Brooks A, Jardim A, López-Mendilaharsu M, González-Paredes D, Estrades A, Fallabrino A, Martínez-Souza G, Vélez-Rubio GM, Boulon RH, Collazo JA, Wershoven R, Hernández VG, Stringell TB, Sanghera A, Richardson PB, Broderick AC, Phillips Q, Calosso M, Claydon JAB, Metz TL, Gordon AL, Landry AM, Shaver DJ, Blumenthal J, Collyer L, Godley BJ, McGowan A, Witt MJ, Campbell CL, Lagueux CJ, Bethel TL, Kenyon L (2017) Ecological regime shift drives declining growth rates of sea turtles throughout the West Atlantic. Glob Change Biol 23:4556–4568. https://doi.org/10.1111/gcb.13712

Brown-Peterson NJ, Krasnec MO, Lay CR, Morris JM, Griffitt RJ (2016) Responses of juvenile southern flounder exposed to Deepwater Horizon oil-contaminated sediments. Environ Toxicol Chem 36:1067–1076. https://doi.org/10.1002/etc.3629

Burnham KP, Anderson DR (2002) Model selection and multimodel inference: a practical information-theoretic approach, 2nd edn. Springer, New York

Caillouet CW (2014) Interruption of the Kemp's ridley population's pre-2010 exponential growth in the Gulf of Mexico and its aftermath: one hypothesis. Mar Turt Newsl 143:1–7

Caillouet CW (2019) Excessive annual numbers of neritic immature kemp's ridleys may prevent population recovery. Mar Turt Newsl 158:1–9

Caillouet CW, Shaver DJ, Landry AM Jr (2015) Kemp's ridley sea turtle (*Lepidochelys kempii*) head-start and reintroduction to Padre Island National Seashore, Texas. Herpetol Conserv Biol 10:309–377

Caillouet CW, Gallaway BJ, Putman NF (2016) Kemp's ridley sea turtle saga and setback: novel analyses of cumulative hatchlings released and time-lagged annual nests in Tamaulipas, Mexico. Chelonian Conserv Biol 15:115–131. https://doi.org/10.2744/CCB-1189.1

Caillouet CW, Raborn SW, Shaver DJ, Putman NF, Gallaway BJ, Mansfield KL (2018) Did declining carrying capacity for the Kemp's Ridley sea turtle population within the Gulf of Mexico contribute to the nesting setback in 2010–2017? Chelonian Conserv Biol 17:123–133. https://doi.org/10.2744/CCB-1283.1

Coleman AT, Pulis EE, Pitchford JL, Crocker K, Heaton AJ, Carron AM, Hatchett W, Shannon D, Austin F, Dalton M et al (2016) Population ecology and rehabilitation of incidentally captured Kemp's ridley sea turtles (*Lepidochelys kempii*) in the Mississippi Sound, USA. Herpetol Conserv Biol 11:253–264

Crain CM, Kroeker K, Halpern BS (2008) Interactive and cumulative effects of multiple human stressors in marine systems. Ecol Lett 11:1304–1315. https://doi.org/10.1111/j.1461-0248.2008.01253.x

Dmitriew CM (2011) The evolution of growth trajectories: what limits growth rate? Biol Rev 86:97–116. https://doi.org/10.1111/j.1469-185X.2010.00136.x

Dormann CF, Elith J, Bacher S, Buchmann C, Carl G, Carré G, Marquéz JRG, Gruber B, Lafourcade B, Leitão PJ, Münkemüller T, McClean C, Osborne PE, Reineking B, Schröder B, Skidmore AK, Zurell D, Lautenbach S (2012) Collinearity: a review of methods to deal with it and a simulation study evaluating their performance. Ecography 36:27–46. https://doi.org/10.1111/j.1600-0587.2012.07348.x

Drinkwater KF, Belgrano A, Borja A, Conversi A, Edwards M, Greene CH, Ottersen G, Pershing AJ, Walker H (2003) The response of marine ecosystems to climate variability associated with the North Atlantic Oscillation. In: Hurrell JW, Kushnir Y, Ottersen G, Visbeck M (eds) Geophysical monograph series. American Geophysical Union, Washington, pp 211–234

DWH NRDA Trustees (2016) Deepwater Horizon Oil spill: final programmatic damage assessment and restoration plan and final programmatic environmental impact statement. Department of Commerce and National Oceanic and Atmospheric Administration

Edwards M, Beaugrand G, Helaouët P, Alheit J, Coombs S (2013) Marine ecosystem response to the Atlantic multidecadal oscillation. PLoS ONE 8:e57212. https://doi.org/10.1371/journal.pone.0057212

Francis R (1990) Back-calculation of fish length: a critical review. J Fish Biol 36:883–902

Gaillard J-M, Loison A, ToÏgo C, Delorme D, Laere GV (2003) Cohort effects and deer population dynamics. Écoscience 10:412–420. https://doi.org/10.1080/11956860.2003.11682789

Gallaway BJ, Gazey WJ, Wibbels T, Bevan E, Shaver DJ, George J (2016) Evaluation of the status of the Kemp's ridley sea turtle after the 2010 Deepwater Horizon oil spill. Gulf Mex Sci 33:192–205

Giannini A, Chiang JCH, Cane MA, Kushnir Y, Seager R (2001) The ENSO teleconnection to the tropical Atlantic Ocean: contributions of the remote and local SSTs to rainfall variability in the topical Americas. J Clim 14:4530–4544. https://doi.org/10.1175/1520-0442(2001)014<4530:TETTTT>2.0.CO;2

Giltz SM, Taylor CM (2017) Sublethal toxicity of crude oil exposure in the blue crab, *Callinectes sapidus*, at two life history stages. Bull Environ Contam Toxicol 98(2):178–182. https://doi.org/10.1007/s00128-016-2000-7

Gower J, Young E, King S (2013) Satellite images suggest a new Sargassum source region in 2011. Remote Sens Lett 4:764–773. https://doi.org/10.1080/2150704X.2013.796433

Greene CH, Meyer-Gutbrod E, Monger BC, McGarry LP, Pershing AJ, Belkin IM, Fratantoni PS, Mountain DG, Pickart RS, Proshutinsky A, Ji R, Bisagni JJ, Hakkinen SMA, Haidvogel DB, Wang J, Head E, Smith P, Reid PC, Conversi A (2013) Remote climate forcing of decadal-scale regime shifts in Northwest Atlantic shelf ecosystems. Limnol Oceanogr 58:803–816. https://doi.org/10.4319/lo.2013.58.3.0803

GSMFC (2015) The blue crab fishery of the Gulf of Mexico: a regional management plan. Gulf State marine fisheries commission, Ocean Springs, MS

Halpern BS, Walbridge S, Selkoe KA, Kappel CV, Micheli F, D'Agrosa C, Bruno JF, Casey KS, Ebert C, Fox HE, Fujita R, Heinemann D, Lenihan HS, Madin EMP, Perry MT, Selig ER, Spalding M, Steneck R, Watson R (2008) A global map of human impact on marine ecosystems. Science 319:948–952. https://doi.org/10.1126/science.1149345

Hart KM, Lamont MM, Sartain AR, Fujisaki I (2014) Migration, foraging, and residency patterns for northern Gulf loggerheads: implications of local threats and international movements. PLoS ONE 9:e103453. https://doi.org/10.1371/journal.pone.0103453

Henderson ME, Mills KE, Thomas AC, Pershing AJ, Nye JA (2017) Effects of spring onset and summer duration on fish species distribution and biomass along the Northeast United States continental shelf. Rev Fish Biol Fish 27:411–424. https://doi.org/10.1007/s11160-017-9487-9

Heppell SS, Caswell H, Crowder LB (2000) Life histories and elasticity patterns: perturbation analysis for species with minimal demographic data. Ecology 81:654. https://doi.org/10.2307/177367

Heppell SS, Crouse DT, Crowder LB, Epperly SP, Gabriel W, Henwood T, Marquez R, Thompson NB (2004) A population model to estimate recovery time, population size and management impacts on Kemp's ridley sea turtles. Chelonian Conserv Biol 4:765–771

Heppell SS, Burchfield PM, Pena LJ (2007) Kemp's ridley recovery: how far have we come, and where are we headed? In: Plotkin PT (ed) Biology and conservation of ridley sea turtles. Johns Hopkins University Press, Baltimore, pp 325–335

Herdter ES, Chambers DP, Stallings CD, Murawski SA (2017) Did the Deepwater Horizon oil spill affect growth of Red Snapper in the Gulf of Mexico? Fish Res 191:60–68. https://doi.org/10.1016/j.fishres.2017.03.005

Hothorn T, Lausen B (2003) On the exact distribution of maximally selected rank statistics. Comput Stat Data Anal 43:121–137. https://doi.org/10.1016/S0167-9473(02)00225-6

Hothorn T, Hornik K, van de Wiel MA, Zeileis A (2006) Coin: conditional inference procedures in a permutation test framework

Karnauskas M, Schirripa MJ, Craig JK, Cook GS, Kelble CR, Agar JJ, Black BA, Enfield DB, Lindo-Atichati D, Muhling BA, Purcell KM, Richards PM, Wang C (2015) Evidence of climate-driven ecosystem reorganization in the Gulf of Mexico. Glob Change Biol 21:2554–2568. https://doi.org/10.1111/gcb.12894

Kellar NM, Speakman TR, Smith CR, Lane SM, Balmer BC, Trego ML, Catelani KN, Robbins MN, Allen CD, Wells RS, Zolman ES, Rowles TK, Schwacke LH (2017) Low reproductive success rates of common bottlenose dolphins *Tursiops truncatus* in the northern Gulf of Mexico following the Deepwater Horizon disaster (2010–2015). Endanger Species Res 33:143–158. https://doi.org/10.3354/esr00775

Kocmoud AR, Wang H-H, Grant WE, Gallaway BJ (2019) Population dynamics of the endangered Kemp's ridley sea turtle following the 2010 oil spill in the Gulf of Mexico: simulation of potential cause-effect relationships. Ecol Model 392:159–178. https://doi.org/10.1016/j.ecolmodel.2018.11.014

Lamont MM, Fujisaki I (2014) Effects of ocean temperature on nesting phenology and fecundity of the loggerhead sea turtle (*Caretta caretta*). J Herpetol 48:98–102. https://doi.org/10.1670/12-217

Lane SM, Smith CR, Mitchell J, Balmer BC, Barry KP, McDonald T, Mori CS, Rosel PE, Rowles TK, Speakman TR, Townsend FI, Tumlin MC, Wells RS, Zolman ES, Schwacke LH (2015) Reproductive outcome and survival of common bottlenose dolphins sampled in Barataria Bay, Louisiana, USA, following the Deepwater Horizon oil spill. Proc R Soc B 282:20151944. https://doi.org/10.1098/rspb.2015.1944

Larsson K, Forslund P (1991) Environmentally induced morphological variation in the Barnacle Goose, Branta leucopsis. J Evol Biol 4:619–636. https://doi.org/10.1046/j.1420-9101.1991.4040619.x

López-Duarte PC, Fodrie FJ, Jensen OP, Whitehead A, Galvez F, Dubansky B, Able KW (2016) Is exposure to Macondo oil reflected in the otolith chemistry of marsh-resident fish? PLoS ONE 11:e0162699. https://doi.org/10.1371/journal.pone.0162699

Luczak C, Beaugrand G, Jaffré M, Lenoir S (2011) Climate change impact on Balearic shearwater through a trophic cascade. Biol Lett 7:702–705. https://doi.org/10.1098/rsbl.2011.0225

Madsen T, Shine R (2000) Silver spoons and snake body sizes: prey availability early in life influences long-term growth rates of free-ranging pythons. J Anim Ecol 69:952–958. https://doi.org/10.1111/j.1365-2656.2000.00477.x

McAdam AG, Boutin S (2003) Effects of food abundance on genetic and maternal variation in the growth rate of juvenile red squirrels. J Evol Biol 16:1249–1256. https://doi.org/10.1046/j.1420-9101.2003.00630.x

McCauley DJ, Pinsky ML, Palumbi SR, Estes JA, Joyce FH, Warner RR (2015) Marine defaunation: animal loss in the global ocean. Science 347:1255641–1255641. https://doi.org/10.1126/science.1255641

McDonald T, Schroeder B, Stacy B, Wallace B, Starcevich L, Gorham J, Tumlin M, Cacela D, Rissing M, McLamb D, Ruder E, Witherington B (2017) Density and exposure of surface-pelagic juvenile sea turtles to Deepwater Horizon oil. Endanger Species Res 33:69–82. https://doi.org/10.3354/esr00771

Meador JP, Sommers FC, Ylitalo GM, Sloan CA (2006) Altered growth and related physiological responses in juvenile Chinook salmon (*Oncorhynchus tshawytscha*) from dietary exposure to polycyclic aromatic hydrocarbons (PAHs). Can J Fish Aquat Sci 63:2364–2376. https://doi.org/10.1139/f06-127

Mills K, Pershing A, Brown C, Chen Y, Chiang F-S, Holland D, Lehuta S, Nye J, Sun J, Thomas A, Wahle R (2013) Fisheries management in a changing climate: lessons from the 2012 ocean heat wave in the Northwest Atlantic. Oceanography. https://doi.org/10.5670/oceanog.2013.27

Mitchelmore C, Bishop C, Collier T (2017) Toxicological estimation of mortality of oceanic sea turtles oiled during the Deepwater Horizon oil spill. Endanger Species Res 33:39–50. https://doi.org/10.3354/esr00758

Müller J, Hothorn T (2004) Maximally selected two-sample statistics as a new tool for the identification and assessment of habitat factors with an application to breeding-bird communities in oak forests. Eur J For Res 123:219–228. https://doi.org/10.1007/s10342-004-0035-5

Murawski S, Fleeger J, Patterson W III, Hu C, Daly K, Romero I, Toro-Farmer G (2016) How did the Deepwater Horizon oil spill affect coastal and continental shelf ecosystems of the Gulf of Mexico? Oceanography 29:160–173. https://doi.org/10.5670/oceanog.2016.80

Musick JA, Limpus CJ (1997) Habitat utilization and migration in juvenile sea turtles. In: Lutz PL, Musick JA (eds) The biology of sea turtles. CRC Press, Boca Raton, pp 137–164

NMFS, Usfws, (2015) Kemp's ridley sea turtle (Lepidochelys kempii) 5-year review: summary and evaluation. National Marine Fisheries Service, Silver Spring

Ogle DH, Wheeler P, Dinno A (2018) FSA: fisheries stock analysis

Parham JF, Zug GR (1997) Age and growth of loggerhead sea turtles (*Caretta caretta*) of coastal Georgia: an assessment of skeletochronological age-estimates. Bull Mar Sci 61:287–304

Perez CR, Moye JK, Cacela D, Dean KM, Pritsos CA (2017) Body mass change in flying homing pigeons externally exposed to Deepwater Horizon crude oil. Ecotoxicol Environ Saf 146:104–110. https://doi.org/10.1016/j.ecoenv.2017.05.012

Pershing AJ, Alexander MA, Hernandez CM, Kerr LA, Le Bris A, Mills KE, Nye JA, Record NR, Scannell HA, Scott JD, Sherwood GD, Thomas AC (2015) Slow adaptation in the face of rapid warming leads to collapse of the Gulf of Maine cod fishery. Science 350:809–812. https://doi.org/10.1126/science.aac9819

Pershing A, Mills K, Dayton A, Franklin B, Kennedy B (2018) Evidence for adaptation from the 2016 Marine heatwave in the Northwest Atlantic Ocean. Oceanography. https://doi.org/10.5670/oceanog.2018.213

Peterson CH, Rice SD, Short JW, Esler D, Bodkin JL, Ballachey BE, Irons DB (2003) Long-term ecosystem response to the Exxon Valdez oil spill. Science 302:2082–2086

Powers SP, Hernandez FJ, Condon RH, Drymon JM, Free CM (2013) Novel pathways for injury from offshore oil spills: direct, sublethal and indirect effects of the Deepwater Horizon oil spill on pelagic *Sargassum* communities. PLoS ONE 8:e74802. https://doi.org/10.1371/journal.pone.0074802

Putman NF, Mansfield KL, He R, Shaver DJ, Verley P (2013) Predicting the distribution of oceanic-stage Kemp's ridley sea turtles. Biol Lett 9:20130345. https://doi.org/10.1098/rsbl.2013.0345

Putman NF, Abreu-Grobois FA, Iturbe-Darkistade I, Putman EM, Richards PM, Verley P (2015) Deepwater Horizon oil spill impacts on sea turtles could span the Atlantic. Biol Lett 11:20150596. https://doi.org/10.1098/rsbl.2015.0596

R Core Team (2019) R: a language and environment for statistical computing

Ramirez MD, Avens L, Goshe LR, Snover ML, Cook M, Heppell SS (2020) Regional variation in Kemp's ridley sea turtle diet composition and its potential relationship with somatic growth. Front Mar Sci 7:253. https://doi.org/10.3389/fmars.2020.00253

Reich KJ, López-Castro MC, Shaver DJ, Iseton C, Hart KM, Hooper MJ, Schmitt CJ (2017) δ^{13}C and δ^{15}N in the endangered Kemp's ridley sea turtle *Lepidochelys kempii* after the Deepwater Horizon oil spill. Endanger Species Res 33:281–289. https://doi.org/10.3354/esr00819

Reid PC, Beaugrand G (2012) Global synchrony of an accelerating rise in sea surface temperature. J Mar Biol Assoc UK 92:1435–1450. https://doi.org/10.1017/S0025315412000549

Renaud ML, Williams JA (2005) Kemp's ridley sea turtle movements and migrations. Chelonian Conserv Biol 4:808–816

Rocha J, Yletyinen J, Biggs R, Blenckner T, Peterson G (2014) Marine regime shifts: drivers and impacts on ecosystems services. Phil Trans R Soc B 370:20130273. https://doi.org/10.1098/rstb.2013.0273

Romero IC, Toro-Farmer G, Diercks A-R, Schwing P, Muller-Karger F, Murawski S, Hollander DJ (2017) Large-scale deposition of weathered oil in the Gulf of Mexico following a deep-water oil spill. Environ Pollut 228:179–189. https://doi.org/10.1016/j.envpol.2017.05.019

Romero IC, Sutton T, Carr B, Quintana-Rizzo E, Ross SW, Hollander DJ, Torres JJ (2018) Decadal assessment of polycyclic aromatic hydrocarbons in mesopelagic fishes from the Gulf of Mexico reveals exposure to oil-derived sources. Environ Sci Technol 52:10985–10996. https://doi.org/10.1021/acs.est.8b02243

Rouhani S, Baker MC, Steinhoff M, Zhang M, Oehrig J, Zelo IJ, Emsbo-Mattingly SD, Nixon Z, Willis JM, Hester MW (2017) Nearshore exposure to Deepwater Horizon oil. Mar Ecol Prog Ser 576:111–124. https://doi.org/10.3354/meps11811

Rozas LP, Minello TJ, Miles MS (2014) Effect of Deepwater Horizon oil on growth rates of juvenile Penaeid shrimps. Estuaries Coasts 37:1403–1414. https://doi.org/10.1007/s12237-013-9766-1

Rudloe A, Rudloe J (2005) Site specificity and the impact of recreational fishing activity on subadult endangered Kemp's ridley sea turtles in estuarine foraging habitats in the northeastern Gulf of Mexico. Gulf Mex Sci. https://doi.org/10.18785/goms.2302.05

Sanchez-Rubio G, Perry HM, Biesiot PM, Johnson DR, Lipcius RN (2011) Climate-related hydrological regimes and their effects on abundance of juvenile blue crabs (*Callinectes sapidus*) in the northcentral Gulf of Mexico. Fish Bull 109:139–146

Sanchez-Rubio G, Perry H, Franks JS, Johnson DR (2018) Occurrence of pelagic *Sargassum* in waters of the U.S. Gulf of Mexico in response to weather-related hydrographic regimes associated with decadal and interannual variability in global climate. Fish Bull 116:93–106

Schwacke LH, Smith CR, Townsend FI, Wells RS, Hart LB, Balmer BC, Collier TK, De Guise S, Fry MM, Guillette LJ, Lamb SV, Lane SM, McFee WE, Place NJ, Tumlin MC, Ylitalo GM, Zolman ES, Rowles TK (2014) Health of Common Bottlenose Dolphins (*Tursiops truncatus*) in Barataria Bay, Louisiana, following the Deepwater Horizon oil spill. Environ Sci Technol 48:93–103. https://doi.org/10.1021/es403610f

Schwacke L, Thomas L, Wells R, McFee W, Hohn A, Mullin K, Zolman E, Quigley B, Rowles T, Schwacke J (2017) Quantifying injury to common bottlenose dolphins from the Deepwater Horizon oil spill using an age-, sex- and class-structured population model. Endanger Species Res 33:265–279. https://doi.org/10.3354/esr00777

Shaver DJ, Hart KM, Fujisaki I, Rubio C, Sartain AR, Peña J, Burchfield PM, Gamez DG, Ortiz J (2013) Foraging area fidelity for Kemp's ridleys in the Gulf of Mexico. Ecol Evol 3:2002–2012. https://doi.org/10.1002/ece3.594

Shaver DJ, Rubio C, Shelby Walker J, George J, Amos AF, Reich K, Jones C, Shearer T (2016) Kemp's ridley sea turtle (*Lepidochelys kempii*) nesting on the Texas coast: geographic, temporal, and demographic trends through 2014. Gulf Mex Sci. https://doi.org/10.18785/goms.3302.04

Snover ML, Hohn AA (2004) Validation and interpretation of annual skeletal marks in loggerhead (*Caretta caretta*) and Kemp's ridley (*Lepidochelys kempii*) sea turtles. Fish Bull 102:682–692

Snover ML, Hohn AA, Crowder LB, Heppell SS (2007) Age and growth in Kemp's ridley sea turtles: evidence from mark-recapture and skeletochronology. In: Plotkin PT (ed) Biology and conservation of ridley sea turtles. Johns Hopkins University Press, Baltimore, pp 89–106

Stacy BA (2015) Summary of necropsy findings for non-visibly oiled sea turtles documented by stranding response in Alabama, Louisiana, and Mississippi 2010 through 2014

Stacy N, Field C, Staggs L, MacLean R, Stacy B, Keene J, Cacela D, Pelton C, Cray C, Kelley M, Holmes S, Innis C (2017) Clinicopathological findings in sea turtles assessed during the Deepwater Horizon oil spill response. Endanger Species Res 33:25–37. https://doi.org/10.3354/esr00769

Stubbs JL, Marn N, Vanderklift MA, Fossette S, Mitchell NJ (2020) Simulated growth and reproduction of green turtle (*Chelonia mydas*) under climate change and marine heatwave scenarios. Ecol Model 431:109185. https://doi.org/10.1016/j.ecolmodel.2020.109185

TEWG (Turtle Expert Working Group) (2000) Assessment update for the Kemp's ridley and loggerhead sea turtle populations in the western North Atlantic

VanderKooy S (2013) Stock assessment report GDAR 01: Gulf of Mexico blue crab. Ocean Springs, MS

Wallace B, Stacy B, Rissing M, Cacela D, Garrison L, Graettinger G, Holmes J, McDonald T, McLamb D, Schroeder B (2017) Estimating sea turtle exposures to Deepwater Horizon oil. Endanger Species Res 33:51–67. https://doi.org/10.3354/esr00728

Wilson RM, Cherrier J, Sarkodee-Adoo J, Bosman S, Mickle A, Chanton JP (2015) Tracing the intrusion of fossil carbon into coastal Louisiana macrofauna using natural 14C and 13C abundances. Deep Sea Res Part II Top Stud Oceanogr. https://doi.org/10.1016/j.dsr2.2015.05.014

Wise JP, Wise JTF, Wise CF, Wise SS, Gianios C, Xie H, Thompson WD, Perkins C, Falank C, Wise JP (2014) Concentrations of the genotoxic metals, chromium and nickel, in whales, tar balls, oil slicks, and released oil from the Gulf of Mexico in the immediate aftermath of the Deepwater Horizon oil crisis: is genotoxic metal exposure part of the Deepwater Horizon legacy? Environ Sci Technol 48:2997–3006. https://doi.org/10.1021/es405079b

Witherington B (2002) Ecology of neonate loggerhead turtles inhabiting lines of downwelling near a Gulf Stream front. Mar Biol 140:843–853. https://doi.org/10.1007/s00227-001-0737-x

Witherington B, Hirama S, Hardy R (2012) Young sea turtles of the pelagic *Sargassum*-dominated drift community: habitat use, population density, and threats. Mar Ecol Prog Ser 463:1–22. https://doi.org/10.3354/meps09970

Wood SN (2006) Generalized additive models: an introduction with R. Chapman and Hall/CRC, Boca Raton

Ylitalo G, Collier T, Anulacion B, Juaire K, Boyer R, da Silva D, Keene J, Stacy B (2017) Determining oil and dispersant exposure in sea turtles from the northern Gulf of Mexico resulting from the Deepwater Horizon oil spill. Endanger Species Res 33:9–24. https://doi.org/10.3354/esr00762

Zeileis A, Leisch F, Hornik K, Kleiber C (2002) Strucchange: an R package for testing for structural change in linear regression models. J Stat Softw 7:1–38

Zug GR, Wynn AH, Ruckdeschel C (1986) Age determination of loggerhead sea turtles, *Caretta caretta*, by incremental growth marks in the skeleton. Smithson Contrib Zool 427:1–44